Microbial dynamics and soil physicochemical properties explain large-scale variations in soil organic carbon

Haicheng Zhang, Daniel S. Goll, Ying-Ping Wang, Philippe Ciais, William R. Wieder, Rose Z Abramoff, Yuanyuan Huang, Bertrand Guenet, Anne-katrin Prescher, Raphael A. Viscarra Rossel, et al.

1

2   DR. HAICHENG   ZHANG (Orcid ID : 0000-0002-9313-5953)

3   DR. WILLIAM R WIEDER (Orcid ID : 0000-0001-7116-1985)

4   DR. BERTRAND   GUENET (Orcid ID : 0000-0002-4311-8645)

5   PROF. RAPHAEL A. VISCARRA ROSSEL (Orcid ID : 0000-0003-1540-4748)

6   DR. GUOYI   ZHOU (Orcid ID : 0000-0002-5667-7411)

7

8

10

11

12   **Microbial dynamics and soil physicochemical properties**

13   **explain large scale variations in soil organic carbon**

14

15   Running Title: Microbe & soil property explain SOC variation

16

17   **Haicheng Zhang[1,2], Daniel S. Goll[1,3], Ying-Ping Wang[4], Philippe Ciais[1], William R. Wieder[5,6],**

18   **Rose Abramoff[1], Yuanyuan Huang[1], Bertrand Guenet[1], Anne-Katrin Prescher[7], Raphael A.**

19   **Viscarra Rossel[8], Pierre Barré[9], Claire Chenu[10], Guoyi Zhou[11], Xuli Tang[11]**

20

21   *[1]Le Laboratoire des Sciences du Climat et de l'Environnement, IPSL-LSCECEA/CNRS/UVSQ Saclay,*

22   *91191, Gif-sur-Yvette, France*

23   *[2]Department Geoscience, Environment & Society, Université Libre de Bruxelles, 1050 Bruxelles,*

24   *Belgium*

25   *[3] Institute of Geography, University of Augsburg, Augsburg, Germany*

26   *[4]CSIRO Oceans and Atmosphere Private Bag 1, Aspendale, Vic 3195, Australia*

27   *[5]Climate and Global Dynamics Laboratory, National Center for Atmospheric Research, Boulder, CO,*

28   *USA*

29   *⁶Institute of Arctic and Alpine Research, University of Colorado, Boulder, CO, USA*

30   *⁷Thünen Institute of Forest Ecosystems, Alfred-Möller-Straße 1, 16225 Eberswalde, Germany*

31   *⁸Soil & Landscape Science, School of Molecular & Life Sciences, Faculty of Science & Engineering,*

32   *Curtin University, Perth, Western Australia, Australia.*

33   *⁹Laboratoire de Géologie de l'ENS, PSL Research University, UMR8538 du CNRS, 24 rue Lhomond,*

34   *75231, Paris, cedex 05, France*

35   *¹⁰UMR ECOSYS, INRA, AgroParisTech, Université Paris-Saclay, 78850 Thiverval-Grignon, France*

36   *¹¹South China Botanical Garden, Chinese Academy of Sciences, Guangzhou 510650, China*

37

38   Correspondence: Haicheng Zhang (haicheng.zhang@lsce.ipsl.fr)

39   Type: primary research

40

41   **Abstract**

42   First-order organic matter decomposition models are used within most Earth

43   System Models (ESMs) to project future global carbon cycling; these models have

44   been criticized for not accurately representing mechanisms of soil organic carbon

45   (SOC) stabilization and SOC response to climate change. New soil biogeochemical

46   models have been developed, but their evaluation is limited to observations from

47   laboratory incubations or few field experiments. Given the global scope of ESMs, a

48   comprehensive evaluation of such models is essential using *in situ* observations of a

49   wide range of SOC stocks over large spatial-scales before their introduction to ESMs.

50   In this study, we collected a set of *in situ* observations of SOC, litterfall and soil

51   properties from 206 sites covering different forest and soil types in Europe and China.

52   These data were used to calibrate the model MIMICS (The MIcrobial-MIneral Carbon

53   Stabilization model), which we compared to the widely used first-order model

54   CENTURY. We show that, compared to CENTURY, MIMICS more accurately

55   estimates forest SOC concentrations and the sensitivities of SOC to variation in soil

56   temperature, clay content and litter input. The ratios of microbial biomass to total

57   SOC predicted by MIMICS agree well with independent observations from

58   globally-distributed forest sites. By testing different hypotheses regarding (by using

59   alternative process representations) of the physicochemical constraints on SOC

60   deprotection and microbial turnover in MIMICS, the errors of simulated SOC

61   concentrations across sites were further decreased. We show that MIMICS can

62   resolve the dominant mechanisms of SOC decomposition and stabilization and that it

63   can be a reliable tool for predictions of terrestrial SOC dynamics under future climate

64   change. It also allows us to evaluate at large scale the rapidly evolving understanding

65   of SOC formation and stabilization based on laboratory and limited filed observation.

66

71   **1 | INTRODUCTION**

72   Soil organic carbon (SOC) is the largest terrestrial carbon (C) pool (Ciais et al.,

73   2013), and contains more than three times as much C as either the atmosphere or

74   terrestrial vegetation. Therefore, a small change (< 1 %) in the global SOC pool might

75   drastically alter the land-atmosphere C balance (Heimann & Reichstein, 2008; Shi et

76   al., 2018). SOC is also closely related to soil fertility, structure, water holding

77   capacity and ecosystem biogeochemical cycles (Six et al., 2004; Campbell & Paustian,

78   2015). Dynamics of SOC have received increasing attention in many research areas

79   ranging from small-scale projects for preserving or improving soil health, to

80   large-scale climate change mitigation (e.g. the "4per1000" initiative) (Lal, 2016). Soil

81   biogeochemical models are the main tools for estimating global land C stock and the

82   interactions between SOC dynamic and changes in climate and land use.

83   The majority of global soil C models are developed based on first-order kinetics,

84   in which the decomposition rate of organic matter is proportional to the pool size and

85   turnover rate, modified by environmental factors (Parton et al., 1987; Manzoni &

86   Porporato, 2009). These models are mathematically simple and stable, and have been

87   proven effective for simulating soil organic matter dynamics (e.g. the decreasing trend

88   of remaining organic matter mass during decomposition experiments, Barré et al.,

89   2010; Bonan et al., 2013). However, these models are unable to mechanically

90   represent the transient SOC dynamics in response to increased fresh litter input

91   (Fontaine et al., 2007; Guenet et al., 2010; Kuzyakov, 2010), likely because they lack

92   explicit representation of microbial decomposition and SOC stabilization (Schmidt et

93   al., 2011; Creamer et al., 2015). Earth System Models (ESMs) which use the

94   first-order soil C models also show poor agreement with global spatial variation of

95   SOC stock (Todd-Brown et al., 2013; Hararuk & Luo, 2014; Wu et al., 2018).

96   Moreover, the conceptual SOC pools used in conventional models are largely not

97   observable (Elliot et al., 1996; Abramoff et al., 2018; Robertson et al., 2019), making

98   it challenging to validate conventional soil C models using field observations (Six et

99   al., 2014; Viscarra Rossel et al., 2019).

100   New theories and soil biogeochemical models have been developed to explicitly

101   represent microbial biomass and physiology (Allison, 2012; Cotrufo et al., 2013;

102   Wieder et al., 2014b; Campbell et al., 2016; Abramoff et al., 2018, 2019; Huang et al.,

103   2018; Robertson et al., 2019). These microbial models are valuable for testing specific

104   responses of SOC at small spatial scales, such as the effect of short-term priming

105   observed during litter manipulation experiments or the addition of labile organic

106   matter to the incubated soil samples in the lab. However, they introduce parameters

107   determined from short term experiments or under laboratory conditions. Thus,

108   microbial models add uncertainty to large-scale simulations (Stockmann et al., 2013;

109   Wang et al., 2014; Shi et al., 2018; Robertson et al., 2019), because most of these

110   models are calibrated against observed litter or SOC decomposition rates obtained

111   from limited laboratory or field experiments (Wieder et al., 2014b; Campbell et al.,

112   2016; Georgiou et al., 2017). Robust datasets which can be used to comprehensively

113   evaluate the simulated quasi-equilibrium SOC pool sizes are still scarce (Wieder et al.,

114   2014a). Furthermore, it remains difficult to determine whether microbial explicit

115   models outperform conventional first-order models on predicting large-scale SOC

116   spatial gradients and temporal dynamics (Campbell & Paustian, 2015; Wieder et al.,

117   2015, 2018). Microbial models have to be carefully calibrated and evaluated before

118   they are used to replace conventional first-order models in ESMs (Wieder et al., 2013;

119   Wang et al., 2014).

120   Several studies have calibrated and validated microbial decomposition models

121   (Wieder et al., 2013, 2015; Robertson et al., 2019) using globally gridded soil

122   databases such as the Harmonized Word Soils Database (HWSD,

123   FAO/IIASA/ISRIC/ISSCAS/JRC, 2012) and the Northern Circumpolar Soil Carbon

124   Database (NCSDC, Tarnocai et al., 2009). However these global databases do not

125   contain uncertainty estimates (Dai et al., 2018), and previous studies have identified

126   significant differences between SOC estimates from these databases or between

127   grid-scale estimates from these databases and point-scale *in situ* observations (Tifafi

128   et al., 2018; Fig. S1 in supplementary material). In addition, there is still no reliable

129   globally gridded database of plant litter input. Uncertainties in the boundary

130   conditions (e.g. litter inputs simulated by ESMs and soil physical and chemical

131   properties) used as model forcing data further hamper the use of these global

132   databases for model evaluation. An alternative approach is to calibrate and evaluate

133   the microbial-explicit SOC models using extensive in situ observations of SOC

134   contents, soil properties, litterfall production and climate conditions. Moreover, to

135   ensure that the tested microbial model can capture many key processes related to SOC

136   decomposition and stabilization, rather than only simulate the total SOC contents, it is

137   necessary to evaluate the simulated composition of different C pools to total SOC, the

138   turnover time of each C pool, and the sensitivity of SOC content to litter input and

139   soil properties.

140   In this study we compiled a large set of *in situ* observations of SOC

141   concentrations for northern forests, as well as related soil property measurements (e.g.

142   texture, bulk density and pH), annual litter input and climate from 206 forest sites

143   distributed across different climate zones of Europe and China. Using this database,

144   we calibrated and evaluated the first-order soil biogeochemical model CENTURY

145   (Parton et al., 1987) and the microbial trait-based model MIMICS (MIcrobial-MIneral

146   Carbon Stabilization, Wieder et al., 2015). To evaluate the simulated SOC

147   composition, we acquired observations of the ratio of microbial biomass to total SOC,

148 and the SOC fractions that represent the different SOC pools in the total SOC stock

149 from sites that are independent from the European and Chinese sites.

150 The aim of this study is to assess the strength and weakness of microbial implicit

151 and microbial explicit models in simulating the stocks and composition of SOC with

152 the intent of guiding future experiments and model developments. Specifically, we: 1)

153 compared CENTURY and MIMICS with observed forest SOC concentrations at the

154 continental scale, and explored the sources of model biases; 2) quantified the

155 sensitivity of CENTURY- and MIMICS-simulated sensitivities of SOC concentration

156 to changing soil conditions and litterfall inputs; 3) evaluated the MIMICS-simulated

157 SOC compositions including ratios of microbial biomass to total SOC and the

158 proportions of different SOC pools using observed values globally; 4) explored the

159 main drivers of the variation in SOC composition. Finally we discussed the

160 implications of our results for SOC modeling at global scales.

161

162 **2 | MATERIALS AND METHODS**

163 **2.1 | Observation data on SOC concentration and soil properties**

164 To calibrate and evaluate both soil C models under a wide range of climate

165 conditions and forest types, we compiled observed SOC concentrations and the

166 corresponding plant biomass, litterfall, soil properties (e.g. bulk density, soil texture,

167 pH) and climate conditions (mean annual temperature) from 72 European forest sites

168 and 134 Chinese forest sites (Fig. S2). The European sites are part of the International

169 Co-operative Programme on Assessment and Monitoring of Air Pollution Effects on

170 Forests (ICP Forests, http://icp-forests.net) operating under the UNECE Air

171 Convention and featuring consistent methods and harmonized data across the whole

172 network (Gleck et al., 2016; Ukonmaanaho et al.,2016). The Chinese forest sites

173 belong to a reviewable and consistent nationwide inventory system established by the

174 Chinese Ministry of Forestry (Tang et al., 2018). The forest stand ages at most sites

175 are older than 40 years. *In situ* observations are mostly conducted during the period

176 from 2000 to 2015, with durations ranging from one to more than 10 years. The

177 observation sites cover four forest types (temperate needle-leaved evergreen forest

178   (TeNE), temperate broad-leaved evergreen forest (TeBE), temperate broad-leaved

179   summer-green forest (TeBS), boreal needle-leaved evergreen forest (BoNE)) and

180   more than 15 soil types (based on the FAO-90 soil classification in HWSD v1.2).

181   Mean annual temperatures of the observation sites span a large range from -10 °C to

182   higher than 20 °C (Fig. S3a). Values of mean annual total precipitation ranged from

183   less than 300 mm yr^{-1} to more than 2000 mm yr^{-1} (Fig. S3b). Annual total litterfall

184   production was between 100 g C m^{-2} yr^{-1} and 2000 g C m^{-2} yr^{-1} (Fig. S3c). Soil

185   properties at the observation sites vary widely (Figs. S3d-i), with soil pH ranges from

186   4.5 to 8.5, and clay fraction ranges from 1% to 45%. Moreover, observation data at

187   European ICP Forest sites provide measurements of SOC concentrations and soil

188   properties at four different layers (0-10, 10-20, 20-40, 40-80 cm) of the top 80 cm soil,

189   whereas data at Chinese sites provide the mean condition of the top 1 m soil.

190   At the European ICP Forest sites, leaf litterfall (including twig litterfall for some

191   sites) was measured *in situ*, but not wood and root litterfall. We estimate the wood

192   litterfall based on the ratios of wood litterfall to leaf litterfall, and the root litterfall

193   based on the root turnover rates and the ratios of root biomass to leaf biomass (Table

194   S1 in supplementary material). At Chinese sites, there are no *in situ* observations of

195   litterfall. We calculated the leaf, wood and root litterfall from observed standing

196   biomass (including leaf, wood and root) and the annual leaf and root turnover rates

197   and the ratios of wood litterfall to leaf litterfall (Table S1). The leaf and root turnover

198   rate, the ratios of wood and root litterfall to leaf litterfall and the ratios of root

199   biomass to leaf biomass used in this study were obtained from a statistical analysis of

200   extensive global observations (Zhang et al., 2014; Holland et al., 2015; Jia et al., 2016,

201   Fig. S4).

202   C:N ratios of leaf litterfall at both European and Chinese sites were measured *in*

203   *situ*. C:N ratios of wood and root litterfall, as well as the litterfall lignin:C ratios for

204   each forest type were obtained from the global Fine-Root Ecology Database (FRED,

205   Iversen et al., 2017) , the TRY database (Kattge et al., 2011) and the Long-Term

206   Inter-site Decomposition Experiment Team (LIDET, Harmon et al., 2009).

207   The soil base saturation (BS, %), Cation Exchange Capacity (CEC, cmol kg^{-1})

208 and soil gravel content (% of volume) at each observation site were obtained from the

209 Global Soil Dataset for Earth System Models (GSDE, Shangguan et al., 2014). Soil

210 type was determined based on the map from HWSD v1.2. Annual mean soil water

211 content (%) was extracted from the estimation of land surface model

212 ORCHIDEE-trunk (r5504, Krinner et al., 2005). LAI and NDVI data were extracted

213 from the GLASS (resolution: 0.05°, Liang et al., 2013) and GIMMS NDVI products

214 (resolution: 8-km, Tucker et al., 2005), respectively. Evapotranspiration (ET) and the

215 potential evapotranspiration (PET) were obtained from Jung et al. (2010) and the

216 CRUNCEP v7 database (Viovy, 2018), respectively. More details of the datasets used

217 in this study can be found in Table S1.

218

219 **2.2 | Decomposition models**

220 **2.2.1 | CENTURY**

221   We selected the CENTURY model (the version presented by Parton et al., 1987)

222 to represent first-order soil biogeochemical models, because it has been widely

223 incorporated into ESMs (e.g. Sitch et al., 2003; Krinner et al., 2005; Koven et al.,

224 2013). In CENTURY, organic matter is separated into metabolic litter (high quality,

225 LIT_m) and structural litter (low quality, LIT_s) and three SOC pools (active pool

226 (SOC_{act}), slow pool (SOC_{slow}), passive pool (SOC_{pas})) with different turnover times

227 (Fig. 1a). Fresh litter inputs are partitioned into metabolic and structural litter pools

228 based on a linear function (f_{met}, dimensionless) of litter lignin to nitrogen (N) ratios

229 (LN) (Parton et al., 1987):

230      $$f_{met} = \max(0.0, 0.85 - 0.013 \times LN) \tag{1}$$

231   There is no explicit representation of microbial biomass in CENTURY. The

232 decomposition of litter and SOC is described by first order kinetics. At each daily

233 time step, the decomposition of litter or SOC (mg C cm^{-3} day^{-1}) is calculated

234 following:

235      $$\frac{dC_s}{dt} = I_c - k_{max} \times C_s \times f(tem) \times f(swc) \times f(clay) \tag{2}$$

236 where C_s (mg C cm^{-3}) is an individual litter or SOC pool, I_c (mg C cm^{-3} day^{-1}) is the C

237 input to the pool considered, k_{max} is the potential maximum turnover rate of C_s (day^{-1})

238 and is equal to the reciprocal of maximum turnover time. $f(tem)$, $f(swc)$ and $f(clay)$ are

239 the soil temperature factor, moisture factor and clay factor modulating decomposition

240 rate, respectively.

241 **2.2.2 | MIMICS** (default and modified versions)

242 *The default version of MIMICS* (*MIMICS-def*)

243 The MIcrobial-MIneral Carbon Stabilization model (MIMICS, Wieder et al.,

244 2014b, 2015) explicitly considers the relationships among litter quality, functional

245 tradeoffs in microbial physiology, and the physical and physicochemical protection of

246 microbial byproducts in forming stable soil organic matter. Like CENTURY,

247 MIMICS also has two types of litter pool: metabolic (LIT$_m$) and structural (LIT$_s$) litter

248 (Fig. 1b), and the method used to partition fresh litter input into metabolic and

249 structural pools (f_{met}, Fig. 1b) is the same as that used in CENTURY (Eq. 1). SOC in

250 MIMICS is divided into three pools: the physically and physicochemically protected

251 (SOC$_p$), the chemically recalcitrant (SOC$_c$) and available (SOC$_a$). Two microbial

252 functional types are represented in MIMICS that roughly correspond to

253 microorganisms with copiotrophic (r-strategy, MIC$_r$) and oligotrophic (k-strategy,

254 MIC$_k$) growth strategies (Fig. 1b). The MIC$_r$ is assumed to have higher growth and

255 turnover rates and prefers to consume more labile litter (LIT$_m$), whereas the MIC$_k$ has

256 relatively lower growth and turnover rates and is more competitive when consuming

257 low-quality litter (LIT$_s$) and chemically recalcitrant SOC (SOC$_c$).

258 C fluxes in MIMICS are simulated at an hourly (h) time step. Decomposition of

259 litter and SOC pools (mg C cm^{-3} h^{-1}) is based on temperature-sensitive

260 Michaelis–Menten kinetics (Schimel & Weintraub, 2003; Allison et al., 2010) through

261 the equation:

262 $$\frac{dC_s}{dt} = I_c - \text{MIC} \times \frac{V_{max} \times C_s}{K_m + C_s}$$ (3)

263 where C_s (mg C cm^{-3}) is a substrate pool (LIT or SOC) and MIC (mg C cm^{-3})

264 corresponds to the biomass of each microbial pool (MIC$_r$ or MIC$_k$). I_c is the C input

265 to the pool considered (mg C cm^{-3} h^{-1}). V_{max} and K_m are the microbial maximum

266   reaction velocity (mg C (mg MIC)$^{-1}$ h^{-1}) and half-saturation constant (mg C cm^{-3}),

267   respectively. They are calculated as:

268    $$V_{max} = e^{V_{slope} \times T + V_{int}} \times av \times V_{mod} \tag{4}$$

269    $$K_m = e^{K_{slope} \times T + K_{int}} \times ak \times K_{mod} \tag{5}$$

270   where T is soil temperature (∘C), V_{mod} and K_{mod} represent the modifications of V_{max}

271   and K_m based on assumptions regarding to microbial functional types, litter chemical

272   quality and soil texture effects, av and ak are the tuning coefficient of V_{max} and K_m,

273   respectively. V_{slope} and K_{slope} are two regression coefficients. V_{int} and K_{int} are the

274   regression intercepts.

275   Decomposition rate of substrates and the microbial growth efficiency (MGE, Fig.

276   1b) determine the growth rate of microbes. The turnover of MIC$_r$ and MIC$_k$ (MIC$_\tau$,

277   mg C cm^{-3} h^{-1}) at each time step is calculated based on their specific turnover rate

278   (k_{mic}, h^{-1}), annual total litterfall input (LIT$_{tot}$, g C m^{-2} yr^{-1}) and f_{met} by following:

279    $$\text{MIC}_\tau = a_\tau \times k_{mic} \times e^{c \times f_{met}} \times \max\left(\min\left(\sqrt{LIT_{tot}}, 1.2\right), 0.8\right) \times \text{MIC} \tag{6}$$

280   where a_τ (=1.0, dimensionless) is a tuning coefficient of k_{mic}. c is the regression

281   coefficients, and its value is 0.3 for MIC$_r$ and 0.1 for MIC$_k$. Turnover of microbial

282   biomass provides C inputs to SOC pools (Fig. 1b). The fractions of microbial residues

283   to different SOC pools are determined by soil clay content (f_{clay}) and the quality of

284   litter inputs (lignin:N), and can be specifically calculated by following:

285    $$f_{rp} = \min\left(1.0, a_1 \times e^{1.3 \times f_{clay}}\right) \tag{7}$$

286    $$f_{kp} = \min\left(1.0, a_2 \times e^{0.8 \times f_{clay}}\right) \tag{8}$$

287    $$f_{rc} = \min\left(1.0 - f_{rp}, a_4 \times e^{a_3 \times f_{met}}\right) \tag{9}$$

288    $$f_{kc} = \min\left(1.0 - f_{kp}, a_5 \times e^{a_3 \times f_{met}}\right) \tag{10}$$

289    $$f_{ra} = 1.0 - f_{rp} - f_{rc} \tag{11}$$

290    $$f_{ka} = 1.0 - f_{kp} - f_{kc} \tag{12}$$

291   where $f_{rp}, f_{kp}, f_{rc}, f_{kc}, f_{ra}$ and f_{ka} represent the fractions of MIC$_r$ and MIC$_k$ residues to

292   SOC$_P$, SOC$_c$ and SOC$_a$, respectively. LN is the lignin:N ratio. a_{1-5} are coefficients and

293　their values in default MIMICS can be found in Table S1 in supplementary materials.

294　In addition to microbial residues, a fraction of inputs ($f_{i,met}$ and $f_{i,stru}$) which bypasses

295　litter and microbial biomass pools is transferred directly to corresponding SOC pools

296　(Fig. 1b).

297　　　The transfer of SOC_p to SOC_a (D, mg C cm^{-3} h^{-1}), which is intended to represent

298　the deprotection of SOC, i.e. desorption of physico-chemically protected SOC from

299　mineral surfaces and/or the breakdown of aggregates de-protecting physically

300　protected SOC, is calculated as a function of soil clay content (f_{clay}) by following:

301　　　$$D = 1.5 \times 10^{-5} \times k_d \times e^{-1.5 \times f_{clay}} \tag{13}$$

302　where k_d (=1.0, dimensionless) is a tuning coefficient of the deprotection rate. Some

303　parameter values of the default MIMICS are provided in Table S1 in supplementary

304　materials. Please see Wieder *et al.* (2014b, 2015) for more details of the structure,

305　algorithms, parameters and underlying assumptions of MIMICS.

306

307　*MIMICS with revised SOC deprotection rate (MIMICS-D)*

308　　　In addition to the default version of MIMICS (MIMICS-def), we also developed

309　and tested a new version of MIMICS (MIMICS-D) that considers the saturation of

310　SOC protected by the mineral matrix (SOC_p). In the MIMICS-def, the deprotection

311　rate of SOC_p in a specific soil was a fixed value determined by the abundance of the

312　soil clay fraction (Eq. 13). However, field and laboratory research suggests that there

313　might be an upper limit, or 'saturation level', in the amount of physicochemically and

314　physically protected SOC that can be held in soil (Six et al., 2002; Stewart et al., 2007;

315　Robertson et al., 2019). Deprotection rate of the SOC protected by the mineral matrix

316　is closely related to this saturation degree (defined as the ratio of existing SOC_p to the

317　soil maximum adsorption capacity; Kothawala et al., 2008; Wang et al., 2013). In this

318　study, we did not calculate the maximum adsorption capacity directly, as it is

319　determined by soil physical and chemical characteristics, and there is still no widely

320　recognized method to calculate it (Lützow et al., 2006; Campbell & Paustian, 2015;

321　Huang et al., 2018), The upper-limit of SOC_p was represented by assuming that the

322 deprotection rate increases exponentially with the pool size of SOC_p:

323 $$D = 1.5 \times 10^{-5} \times k_d \times e^{-1.5 \times f_{clay}} \times e^{k_{dp} \times SOC_p} \qquad (14)$$

324 where k_{dp} is a coefficient for tuning the relationship between the deprotection rate (D)

325 and the pool size of SOC_p.

326

327 *MIMICS considering the impact of base saturation (BS) on deprotection rate*

328 (*MIMICS-DB*)

329   We tested several new modifications of MIMICS to see if the inclusion of soil

330 chemical properties (BS and pH) could further decrease the uncertainties in simulated

331 SOC concentrations. We modified the microbial maximum reaction velocity (V_{max}, Eq.

332 4), the C input rates to SOC_p (f_p and $f_{i,met}$ in Fig. 1b) and the deprotection rate of SOC_p

333 with some simple linear or exponential functions of soil BS and pH, separately. In this

334 study, we only present the results from the modification called MIMICS-DB, where

335 the modified deprotection rate of SOC_p is calculated as:

336 $$D = 1.5 \times 10^{-5} \times k_d \times e^{-1.5 \times f_{clay}} \times e^{k_{dp} \times SOC_p} \times e^{k_{bs} \times BS} \qquad (15)$$

337 where k_{bs} is a coefficient modifying the impacts of BS on the deprotection rate.

338

339 *MIMICS considering density-dependent microbial turnover rate (MIMICS-DBT)*

340   Following the method of Georgiou et al. (2017), we also incorporated a

341 density-dependent microbial turnover rate into MIMICS. In this version

342 (MIMICS-DBT), microbial turnover rate increases with growing microbial biomass

343 density (MIC, mg C cm^{-3}) by modifying Eq. 6:

344 $$MIC_\tau = a_\tau \times k_{mic} \times e^{c \times f_{met}} \times \max\left(\min\left(\sqrt{LIT_{tot}}, 1.2\right), 0.8\right) \times (MIC)^\beta$$

345 $$(16)$$

346 where β is the density-dependence exponent.

347

348 **2.3 | Model parameterization and validation against SOC concentrations**

349   We assumed that all the forest sites included in this study are at steady state (i.e.

350 no interannual variation of SOC, litterfall and stand biomass). CENTURY and the

351   four versions of MIMICS introduced above (Table 1) were then calibrated and

352   evaluated against the 'equilibrium' SOC concentrations using observation data of soil

353   texture, annual total litterfall and mean annual temperature. We also ignored the

354   interannual and seasonal dynamics of climate and vegetation. Historical climate,

355   litterfall input and soil properties were all assumed to be similar to the average

356   condition during the observation period. Vertical discretization in SOC and soil

357   properties is not considered in CENTURY and MIMICS. We focus only on the spatial

358   variation of average SOC concentrations in the upper soil horizons (0-80 cm for

359   European sites and 0-1 m for Chinese sites). The semi-analytic approach was used to

360   calculate the steady state microbial and soil C pool sizes (Xia et al., 2012) based on

361   annual total litterfall production (evenly distributed to each time step of simulation),

362   annual mean soil temperature and moisture conditions and observed soil properties at

363   each forest site.

364   Parameters of CENTURY and MIMICS were optimized against the observed

365   SOC concentrations (Table 1). Although many parameters (e.g. carbon use efficiency

366   and parameters related to the constraints of temperature and soil clay on C

367   decomposition rate) of CENTURY and MIMICS can impact the simulated SOC

368   concentrations, we only optimized the parameters which directly control the organic

369   matter decomposition rates. Because these parameters generally contain large

370   uncertainties and the simulated SOC stocks are generally more sensitive to these

371   parameters than to other model parameters (Wieder et al., 2014b, 2015; Shi et al.,

372   2018). Specifically, we added two scaling parameters k_{litt} and k_{soc} (dimensionless) in

373   CENTURY to tune the turnover rates of litter and SOC pools, respectively.

$$374 \qquad k_{max\_litt\_opt} = k_{litt} \times k_{max\_litt} \qquad\qquad (17)$$

$$375 \qquad k_{max\_soc\_opt} = k_{soc} \times k_{max\_soc} \qquad\qquad (18)$$

376   where k_{max_litt} and $k_{max\_litt\_opt}$ are the default and optimized litter turnover rates,

377   respectively. k_{max_soc} and $k_{max\_soc\_opt}$ are the default and optimized SOC turnover rates,

378   respectively. The default litter and SOC turnover rates (see Table S2) were obtained

379   from Parton et al. (1987). Optimization of only k_{litt} and k_{soc} may be not enough to

380   minimize the uncertainties in the turnover rates of litter and SOC pools and the

381   simulated SOC concentrations. We therefore also tested the effectiveness of

382   CENTURY on capturing observed SOC concentrations when five free parameters

383   were introduced to tune the turnover rates of metabolic litter, structural litter, active

384   SOC, slow SOC and passive SOC, respectively (Fig. S5).

385   For the MIMICS models, we optimized the scaling parameters (av, ak and k_d) of

386   the microbial maximum reaction velocity (V_{max}, Eq.4), half-saturation constant (K_m,

387   Eq. 5) and of the deprotection rate of SOC_p (Eqs. 13-15), as they are all closely

388   related to the decomposition and the physical stabilization of organic matter (Wieder

389   *et al.*, 2014b, 2015). Parameters in the newly introduced equations (Eqs. 14-16) for

390   modifying deprotection rates and microbial turnover rate were also optimized (Table

391   1).

392   Parameter optimization was performed using the shuffled complex evolution

393   (SCE) algorithm developed by Duan et al. (1993, 1994), which has proven to be

394   effective for global optimization by many previous studies (e.g. Muttil &

395   Jayawardena, 2008; Franchini et al., 2009). Prior value and the range of each

396   parameter used for the SCE algorithm are listed in Table S3. Root mean square error

397   (RMSE, Eq. 19) between simulated (SOC_{sim_i}) and observed (SOC_{obs_i}) SOC

398   concentrations (g C kg^{-1} soil) was used as the objective function, and parameters that

399   minimized the RMSE were regarded as optimal.

400
$$RMSE = \sqrt{\left(\frac{\sum_{i=1}^{n}(SOC_{obs\_i} - SOC_{sim\_i})^2}{n}\right)} \qquad (19)$$

401   where n is the number of observation sites. In addition to RMSE, the Akaike

402   information criterion (AIC, Eq. 20), which considers both the goodness of fit and

403   the number of free model parameters (n_{param}) were also used to evaluate the

404   optimized models (Table 1).

405
$$AIC = n \times ln\left(\frac{\sum_{i=1}^{n}(SOC_{obs\_i} - SOC_{sim\_i})^2}{n}\right) + 2n_{param} \qquad (20)$$

406   Our preliminary-analyses indicated that parameter optimizations of MIMICS

407   based solely on observed SOC concentration might result in unrealistic estimates of

408   SOC composition (e.g. the SOC_p pool approaching to zero at all sites) and of turnover

409 rates (e.g. the SOC_p turnover rates being significantly larger than SOC_a), although the

410 simulated concentrations of total SOC agreed well with the observations. To mitigate

411 this problem, some additional constraints on simulated SOC composition and turnover

412 rates were incorporated into our optimization scheme (see below). Parameter sets that

413 did not meet the imposed constraints on SOC composition and turnover rates were

414 excluded. Note that the simulated turnover rates of different SOC pools from

415 CENTURY are always consistent with the definition of SOC pools (i.e. the active

416 pool has the largest turnover rate, followed by the slow pool, and the passive pool has

417 the lowest turnover rate), and the simulated SOC composition (mainly determined by

418 the turnover rate of each pool, see section 3.2) did not show any 'abnormalities' (i.e.

419 no simulated SOC pool declined to very small values approaching zero), so we did

420 not incorporate additional constraints when optimizing the parameters of CENTURY.

421 Previous studies suggest that the organic C associated with soil minerals or stored

422 within soil aggregates, corresponding to the SOC_p pool of MIMICS, is the most stable

423 fraction of SOC with turnover times approaching hundreds to thousands of years.

424 Further, the recalcitrant SOC fractions composed by structurally complex compounds

425 corresponding to the SOC_c pool of MIMICS generally have longer turnover time than

426 the labile SOC fraction (Benbi *et al.*, 2014; Robertson *et al.*, 2019; Sokol *et al.*, 2019).

427 Therefore, we set a constraint that the simulated mean SOC_p turnover time for all of

428 the 206 observation sites must be longer than that of SOC_c, and that the mean SOC_c

429 turnover time must be longer than SOC_a.

430 Observations found that a large fraction (e.g. 10-50%) of SOC is in stable pool

431 (Lützow et al., 2007; Barré et al., 2010; Benbi et al., 2014; Viscarra Rossel et al,

432 2019). To avoid the optimized parameters giving a very low (approaching to zero)

433 estimate of the fraction of SOC_p, we also added as a constraint of model results with

434 optimized parameters that the simulated average proportion of SOC_p at the 206

435 observation sites (not for every individual site) must be larger than 5%, that average

436 proportion of SOC_c cannot exceed 70%, and that the total amount of SOC_p and SOC_c

437 should be higher than SOC_a.

438 Note that the parameters (a_{1-5} in Eqs. 7-10) controlling the partition of microbial

439 residues to different SOC pools were modified before the parameters listed in Table 1

440 are optimized, because MIMICS did not give reasonable estimates of the SOC

441 concentrations, compositions and the turnover rates simultaneously when only the

442 parameters listed in Table 1 were calibrated. The modified values of a_{1-5} are provided

443 in Table S2.

444   To explore the sources of simulation errors (i.e. the difference between simulated

445 and observed SOC concentrations), we first calculated the partial correlation

446 coefficient between the errors of the simulated SOC concentration and different soil

447 (e.g. texture, pH, BS and CEC), plant (NDVI and LAI) and climate (temperature,

448 precipitation, ET) variables (see section 2.1 and Table S1 for the source of each

449 variable). Then we fitted a linear mixed-effects (LME) model to quantify the

450 combined contribution of the fixed-effects (soil, plant and climate variables listed

451 above) and site-specific random-effects (e.g. soil type, forest type, stand age and

452 micro-topography) on explaining the simulation errors. All the important variables

453 that might potentially affect SOC dynamics, for example soil texture, temperature, pH,

454 moisture, BS, CEC, bulk density, litterfall inputs, precipitation and ET, were included

455 as fixed-effects in the LME. Observation site was used as a random-effect. We also

456 fitted a multiple linear regression (MLR) with all of the fixed-effects of the LME as

457 the predictor variables to quantify the relative contributions of fixed- and

458 random-effects to the simulation errors. Then the relative contributions of fixed- and

459 random-effects were quantified based on the coefficient of determination of the LME

460 (R^2_{LME}) and MLR (R^2_{MLR}). The contributions of model choice (f_{model}), fixed-effects

461 (f_{fixed}) and random-effects (f_{random}) to explaining the variation of SOC concentrations

462 can be quantified by:

463
$$f_{model} = R^2_{model} \tag{21}$$

464
$$f_{fixed} = R^2_{MLR} \times \left(1 - R^2_{model}\right)$$

465
$$\tag{22}$$

466
$$f_{model} = \left(R^2_{LME} - R^2_{MLR}\right) \times \left(1 - R^2_{model}\right) \tag{23}$$

467 where R^2_{model} is the determining coefficient of the regression equation between

468   simulated and observed SOC concentrations.

469 **2.4 | Model evaluation against sensitivities of SOC concentrations to key model**

470 **drivers**

471   To assess whether each model simulated the variations of SOC concentrations for

472 the right reasons, we first identified the key drivers of the spatial variations of SOC

473 concentration, and then compared modeled sensitivities of SOC concentration to these

474 drivers to the values derived from the observations. The potential key drivers we

475 evaluated include soil temperature, moisture, clay content, litterfall input, the mean

476 C:N ratio and the lignin:C ratio of litterfall. The sensitivities of organic matter

477 decomposition rate to manipulated soil temperature, moisture and litter inputs have

478 been widely investigated via laboratory and field experiments (Parton et al., 2007;

479 Bonan et al., 2013; Sierra et al., 2015). However, no experiments have measured the

480 sensitivity of equilibrium SOC stock to changing soil properties and litter inputs, as it

481 would take decades to hundreds of years for the SOC pool to reach equilibrium after

482 manipulating litter. Here we estimated the sensitivities by making use of observed

483 spatial variation of SOC with different drivers, including soil temperature, water

484 content, clay fraction, annual total litter input and the C:N ratio and lignin:C ratio of

485 litter input. We assumed the soil-litter system is in steady-state, and the sensitivities of

486 equilibrium SOC to different drivers were quantified by multiple linear regression.

487 The regression coefficient of each driver was regarded as the observed sensitivity.

488   The sensitivities of simulated SOC concentration to soil and litter properties from

489 optimized CENTURY and MIMICS were obtained using Monte Carlo simulations.

490 We sampled 1000 sets of unique soil and litter input condition within the observed

491 space of each variable using Latin Hypercube technique (Tang & Zhuang, 2009). All

492 soil and litter variables were assumed to be uniformly distributed and the range of

493 each variable was set based on the maximum and minimum observed values at the

494 European and Chinese sites. For each combination of soil and litter input condition,

495 the sensitivity (S_i) of SOC concentration to each variable (d_i) was calculated as

496 $$S_i = \frac{f(d_1, d_2, \cdots, d_i + \delta, \cdots d_n) - f(d_1, d_2, \cdots, d_i, \cdots d_n)}{\delta}$$

497

498   where δ is the step size of a change in variable d_i assumed to be one percent of the

499   difference between maximum and minimum d_i (i.e. $\delta = (d_{i\_max}-d_{i\_min})/100$).

500

501   **2.5 | Model evaluation against SOC composition**

502   We evaluated the simulated proportions of the different SOC pools using

503   observations from sites that are independent of the European and Chinese forest sites,

504   for which the model parameters were calibrated. The simulated ratios of microbial

505   biomass to total SOC were validated against 655 observations from forest sites around

506   the world (Xu et al., 2013). The simulated SOC composition from CENTURY and

507   MIMICS was compared to measurements of SOC composition from 505 sites under

508   native forests and grasslands in Australia (Viscarra Rossel & Hicks, 2015; Viscarra

509   Rossel et al. 2019). These data were partitioned into three fractions, the particulate

510   organic C (POC), humic organic C (HOC) and resistant organic C (ROC, which is the

511   mineral-associated organic carbon) based on the particle size and chemical

512   compositions of organic matter. We acknowledge the fact that the observed pools are

513   not modeled conceptual pools and we propose a correspondence between both in

514   Table S4. We compared the simulated SOC pools to the observed SOC fractions to

515   assess their correspondence in terms of their expected/assumed turnover rates.

516   **2.6 | Model evaluation against the key drivers of variations in SOC composition**

517   To determine whether the key drivers of variations in SOC composition in

518   MIMICS and CENTURY models are consistent with the observations, we calculated

519   the partial correlation coefficient between fraction of each SOC pool and different

520   model drivers using the simulated proportions of different SOC pools by optimized

521   MIMICS and CENTURY models at all of the 206 forest sites in Europe and China

522   (Fig. S2), and using the observed proportions of different SOC pools at the 505

523   Australia sites (Viscarra Rossel et al. 2019). The key drivers we considered in this

524   analysis include soil temperature, moisture, clay fraction, BS, annual litterfall input,

525   litter C:N and lignin:C ratios and the total SOC pool size). For each model driver, all

526   of the other drivers described above were used as the controlling factor for calculating

527 the partial correlation coefficient.

528

529 **3 | RESULTS**

530 **3.1 | Evaluation of simulated SOC concentrations**

531 Our evaluation indicates that MIMICS can better capture the observed spatial

532 variation of SOC concentrations than CENTURY across European and Chinese forest

533 sites. The default version MIMICS-def explains 48% observed SOC spatial variation,

534 as compared to only 10% by CENTURY model (Fig. 2). MIMICS-D, MIMICS-DB

535 and MIMICS-DBT explain 52%, 57% and 59% SOC spatial variation, respectively

536 (Fig. 2). The RMSE and Akaike information criterion (AIC) indicate that all MIMICS

537 versions estimate the spatial variation of SOC concentration more accurately than

538 CENTURY, with MIMICS-DBT having the best performance overall (Fig. 2f). We

539 also note that the CENTURY model with 5 free parameters for tuning turnover rates

540 of litter and SOC pools (Fig. S5a) does not estimate SOC concentrations more

541 accurately than the CENTURY with 2 free parameters (Table 1). CENTURY with 5

542 free parameters has a slightly smaller RMSE (16.89) but a higher AIC (1174.7) than

543 the RMSE (16.97) and AIC (1170.5) respectively from CENTURY with 2 parameters

544 (Fig. S5a).

545 There are systematic biases in the simulated SOC concentrations along the

546 gradients of SOC pool size, soil properties, and climate and plant variables (Figs. 3

547 and S6). Both CENTURY and MIMICS overestimate the low SOC concentrations but

548 underestimate the high concentrations (Figs. 2 and S6). The simulation biases of

549 CENTURY are significantly correlated with soil (e.g. moisture, BS, pH, and bulk

550 density), plant (e.g. litterfall, LAI) and climate (e.g. mean annual temperature and

551 annual total precipitation) variables (Fig. 3), suggesting that CENTURY has structural

552 biases in the processes depending upon those factors. Similar to CENTURY, the

553 simulation bias of MIMICS is also significantly correlated with some soil and

554 litterfall-related variables. By including the effect of BS on deprotection rate into

555 MIMICS (MIMICS-DB), the significant relationships between simulation biases and

556 soil, plant and climate variables are largely eliminated, but a significant negative

557 relationship between simulation biases and soil CEC appears. The significant

558 relationship between simulation biases and annual litterfall input can be eliminated

559 only when the density dependence of microbial turnover rate in MIMICS-DBT is

560 represented. Moreover, the simulation biases of all models are positively related to

561 soil bulk density (Fig. 3).

562   Soil properties, litter input rate and the plant and climate conditions together can

563 only explain a small portion of the simulation biases in SOC concentrations,

564 especially for MIMICS (Figs. S7, S8). The linear mixed-effects (LME) models which

565 consider both fixed factors (i.e. the soil, litter and climate variables) and site-specific

566 random factor (e.g. soil type, forest type, stand age and micro-topography) explain

567 most of the variations in the simulation biases (Fig. S7). Further statistics indicated

568 that the SOC variation explained by CENTURY, fixed factors and random factors are

569 10%, 27% and 54%, respectively (Fig. S8). But for MIMICS, the model itself

570 explained the largest part (48-59%) of SOC variation, followed by the random factor

571 (24-32%), with fixed factors explaining 5-9% of SOC variation (Fig. S8). Our further

572 analysis on the potential contributors to random factors indicated that CENTURY

573 estimations of SOC are consistently biased regardless of soil type, plant type and

574 stand age (Fig. S9). But the estimations of SOC made by MIMICS are, with few

575 exceptions, unbiased across sites with different soil types, plant types and stand ages.

576 Overall, the constraints of soil, litter and climate factors on SOC stocks are

577 significantly better represented in MIMICS than in CENTURY.

578 **3.2 | Evaluation of simulated sensitivities of SOC concentration to key model**

579 **drivers**

580   Based on observations, SOC concentrations are sensitive to local soil temperature

581 and soil clay content (Figs. 4a, c), but are not sensitive to local soil moisture or litter

582 quantity and quality (Figs. 4b, d, e, f). On average, SOC concentration declines by

583 0.53 g C kg^{-1} soil with a 1 °C increase in soil temperature, and increases by 0.37 g C

584 kg^{-1} soil with a 1 percent increase in soil clay fraction.

585   MIMICS models provide more accurate estimates of the observation-based partial

586 sensitivity of SOC concentration to changes in soil temperature, compared to

587 CENTURY (Fig. 4a). With a 1 °C increase in soil temperature, the simulated SOC

588 concentration declines by 0.4-0.55 g C kg^{-1} soil (median value) depending on the

589 version of MIMICS. The sensitivity is comparable to the value calculated based on

590 observation data, but significantly lower than the value simulated by CENTURY

591 (-0.92±4.1 g C kg^{-1} soil °C^{-1}). Both CENTURY and MIMICS underestimate the

592 observed sensitivity of SOC to soil clay fraction. Despite this, the sensitivities

593 estimated by MIMICS (0.17 – 0.26 g C kg^{-1} soil (clay%)$^{-1}$) are closer to the observed

594 value than CENTURY (0.02 g C kg^{-1} soil (clay%)$^{-1}$, Fig. 4c). In CENTURY or

595 MIMICS, the sensitivities of SOC concentration to these variables generally show

596 large variations. Overall, SOC simulated by CENTURY is more sensitive to the

597 changes in soil condition and litter input than MIMICS.

3.3 | Evaluation of simulated SOC composition

599   The simulated ratios of microbial biomass (MIC) to total SOC stock (MIC/SOC)

600 from the MIMICS models is broadly consistent with the observations collected from

601 global forest sites (Xu *et al*., 2013), both in terms of mean (or median) value and the

602 range of variation (Fig. 5). Overall, both observed and simulated MIC/SOC ranged

603 from 0.005 to approximately 0.05, with a mean value of approximately 0.017

604 (0.015-0.019) and a median value of 0.013 (0.012-0.014).

605   MIMICS simulated fractions of SOC pools that are consistent with measurements

606 of the Australian soil samples based on the particle size and chemical compositions of

607 organic matter (Table S4), but CENTURY did not (Fig. 6). Observations at 505

608 Australian sites indicate that HOC (46-60%) accounts for the largest proportion of

609 SOC, followed by the most stable pool ROC (25-33%). The labile pool POC makes

610 up a small fraction (12-23%) of total SOC (Fig. 6a). MIMICS predicts a similar

611 composition of SOC pools. The moderately stable pool (SOC$_c$) accounts for the

612 largest proportion of total SOC, followed by the most stable pool protected by the

613 mineral matrix (SOC$_p$), and the available pool (SOC$_a$, Fig. 6c). SOC composition

614 simulated by CENTURY can be very different depending on the optimized turnover

615 rates of the active, slow and passive SOC pools (Figs. 6b and S5b). Increasing

616 turnover rate of a specific SOC pool generally results in a smaller proportion of this

617 pool compared to the total SOC (if the turnover rates of other SOC pools are assumed

618 to be fixed).

619 **3.4 | Key drivers of the variation in SOC composition**

620   The key factors controlling the simulated SOC composition in CENTURY and

621 MIMICS are different from the observations (Fig. 7). Based on observation data, soil

622 moisture, clay fraction, BS and litter input show significant empirical correlations

623 with SOC composition, whereas soil temperature shows no significant correlation. In

624 both CENTURY and MIMICS, soil temperature strongly affects SOC composition.

625 Higher temperature however decreases the 'stable' SOC fraction (SOC_{pas}) in

626 CENTURY, but increases the stable fraction (SOC_p) in MIMICS. MIMICS can

627 represent the impacts of litter input on SOC composition, but CENTURY does not.

628 Similar to the observations, higher litter input rate increases the proportion of the

629 stable SOC pools (ROC and SOC_p) but decreases the proportion of moderately stable

630 pools (HOC and SOC_c). The simulated decreasing trend of labile SOC (SOC_a) with

631 increasing litter input is contrary to the observation (POC). In MIMICS-DB and

632 MIMICS-DBT, soil chemical properties represented by BS also show strong impact

633 on SOC composition. Moreover, SOC composition also changes with the pool size of

634 total SOC. It is necessary to note that the partial correlation coefficients might not be

635 able to fully represent the relationships between SOC composition and soil and litter

636 variables (Fig. 7), as SOC composition might not be linearly related to these variables

637 (Fig. S10).

638 **4 | DISCUSSION**

639   Using *in situ* observations of SOC, litterfall and soil properties from 206 forest

640 sites in Europe and China, we compared the performance of a first-order soil

641 biogeochemical model (CENTURY) and four different versions of the microbial

642 trait-based model (MIMICS) for simulating the large-scale spatial variation of SOC

643 concentrations, the sensitivity of SOC concentration to key model drivers and the

644 SOC composition. Our evaluation provides strong evidence that soil biogeochemical

645 models with explicit microbial processes can be applied to simulate the large-scale

646 SOC dynamics across different soil, vegetation and climate conditions. Below we

647   discuss in detail the implications of these results, uncertainties associated with the

648   analysis, and an outlook for future data and model needs.

649   **4.1 | Implications of simulation results**

650   **4.1.1 | Decomposition model should be calibrated and evaluated comprehensively**

651   This study reveals the necessity to calibrate and evaluate MIMICS

652   comprehensively. Preliminary parameter estimates for this study showed that although

653   parameters optimized based solely on observed SOC concentrations can accurately

654   estimate total SOC stocks; they may not be able to estimate SOC composition and

655   turnover time. In order to avoid unreasonable estimates of SOC composition (e.g.

656   SOC_p of MIMICS calibrated only against the SOC concentrations at European and

657   China forest sits always approaches to zero) and C turnover times, we imposed

658   additional constraints to restrict the ranges of proportions and turnover times of

659   MIMICS SOC pools (see section 2.3). Our results highlight the need for comparing

660   model results with total SOC and microbial biomass, SOC composition and turnover

661   time, as well as the response of SOC to changed climate, litter input and soil

662   properties with a wide range of observations. Moreover, the optimized parameter

663   values of both CENTURY and MIMICS in this study (Table S3) are different from

664   the default values calibrated against manipulated decomposition experiments (Parton

665   et al., 1987; Wieder et al., 2015), suggesting that model parameters obtained based on

666   local decomposition experiments might not work well at large spatial scales.

667   **4.1.2 | Importance of explicitly representing microbial dynamics in**

668   **decomposition model**

669   Explicit representation of microbial biomass and substrate-limited growth rates is

670   important for soil biogeochemical models to accurately capture the observed SOC

671   concentration variations and the responses of SOC to climate changes (Wieder et al.,

672   2014b; Campbell & Paustian, 2015). In our research, simulations of SOC

673   concentration at forest sites using MIMICS were more accurate and parsimonious

674   compared to using CENTURY (Fig. 2), and MIMICS better capture the observed

675   sensitivities of SOC concentrations to temperature and soil clay than CENTURY.

676   Conventional first-order models do not explicitly simulate microbial activity, but

677 instead strongly emphasizes the relationship between litter chemical recalcitrance and

678 soil C stock (Jenkinson & Rayner, 1977; Parton et al., 1987; Wieder et al., 2014b).

679 Recent analytical and experimental advances have demonstrated that molecular

680 structure alone does not control SOC stability. Rather, microbial products of

681 decomposition are the main precursors of stable SOC (Cotrufo et al., 2013;

682 Kallenbach et al., 2016), suggesting that, in fact, environmental and biological

683 controls predominate (Lützow et al., 2006; Schmidt et al., 2011; Lehmann & Kleber,

684 2015).

685 **4.1.3 | Impacts of soil physiochemical properties on SOC decomposition and**

686 **stabilization**

687   Besides microbial dynamics, it is also necessary to accurately represent the effects

688 of soil physiochemical properties on SOC dynamics in soil biogeochemical models,

689 especially for the formation and release of SOC protected by the mineral matrix. It

690 has been widely recognized that soil clay fractions can influence SOC stock and

691 stabilization by promoting the sorption of organic C to mineral surfaces and

692 entrapment into micropores (Schimel et al., 1994; Wagner et al., 2007). CENTURY

693 uses the soil clay fraction to modify the decomposition rate of the active SOC pool

694 and the C transfer from active to slow pool (Parton et al., 1987). As the active pool

695 generally accounts for only a small fraction (c.a. 3.5%) of total SOC (Fig. 6b), this

696 might explain why the sensitivity of SOC concentration to soil clay content in

697 CENTURY is drastically underestimated compared to the observation-based

698 sensitivity (Fig. 4c). In MIMICS, soil clay influences both the decomposition rate of

699 available SOC pool and the deprotection rate of protected by the mineral matrix.

700 MIMICS thus better represents current understanding of SOC stabilization processes

701 and appears to more accurately estimate the sensitivity of SOC to soil clay fraction

702 than CENTURY (Fig. 4c).

703   Numerous experimental studies also reported the significant impacts of soil

704 chemical properties such as pH, exchangeable cations (e.g. Ca^{2+}) and extractable

705 metals (e.g. iron- and aluminum-oxyhdroxides) on SOC dynamics (Six et al., 2004;

706 Doetterl et al., 2015; Rasmussen et al., 2018; ViscarraRossel et al., 2019), and the

707   relative importance of these factors likely varies across scales and ecosystems

708   (Jobbágy & Jackson, 2000; Schmidt et al., 2011; ViscarraRossel et al., 2019). Indeed,

709   representing the diversity of mechanisms by which the soil physicochemical

710   environment influences the persistence of soil organic matter in numerically tractable

711   ways remains an outstanding challenge in models (Bailey et al. 2018). Our work

712   suggests one opportunity to use base saturation (BS) as a proxy variable that can

713   modify C deprotection rates from the SOC_p pool in MIMICS (MIMICS-DB). This

714   modification significantly decreased the biases in simulated SOC concentrations (Fig.

715   2) and eliminated the systematic estimation biases along gradients of soil pH, clay

716   content and annual precipitation at the observation sites (Fig. 3). Moreover, our

717   analysis on the relative contributions of model choice, fixed effects and site-specific

718   random effects to explaining the SOC variation (Fig. S8) reveals that the constraints

719   of soil physical (e.g. temperature and clay content) and chemical (e.g. BS) properties

720   on SOC dynamics has been better represented in MIMICS than in CENTURY, as the

721   fixed effects including all potentially important soil variables can only explain a small

722   part of the simulation errors of MIMICS, but a considerable part (~ 30%) of the

723   simulation errors of CENTURY (Fig. S7, S8).

724   **4.1.4| Impacts of litter inputs on SOC decomposition and stabilization**

725   First order models like CENTURY assume a linear relationship with productivity

726   and soil C stocks (Todd-Brown et al. 2013), and the same is true for default

727   parameterizations of MIMICS. Our analysis shows that the simulated SOC

728   concentrations from CENTURY and MIMICS models are systematically biased from

729   observations along the gradients of local litterfall production, except for the

730   MIMICS-DBT which considers the density-dependent turnover of microbes (Fig. 3).

731   This suggests that at the community level, regulatory mechanisms like competition,

732   space constraints and other controls that depend on the density of individuals (such as

733   disease and production of toxins) may limit microbial population sizes (Hibbing et al.,

734   2010; Kaiser et al., 2014; Kaiser et al., 2015) Indeed, a recent study from Georgiou et

735   al. (2017) indicated that the density-dependent microbial processes can play an

736   essential, but often overlooked role in regulating SOC dynamics. We recognize that

737 the parameterization of density dependent turnover implemented in MIMCS-DBT

738 simplifies the complex community interactions that occur in soils, but they represent a

739 tractable means for capturing the emergent dynamics in models that are intended for

740 global-scale application and projections.

741 Litter input is not as important as soil physicochemical properties for predicting

742 total SOC stock (Fig. 4d), but it nevertheless strongly affects SOC composition (Fig.

743 7), which determines the vulnerability of SOC (i.e. risk of C loss) to perturbations

744 such as climate change and human disturbances. Litter quality can impact microbial C

745 use efficiency and short-term SOC dynamics (Manzoni et al., 2017; Zhang et al.,

746 2018), but evidence is inclusive on the significant role of litter quality in long-term

747 SOC dynamics (Helfrich et al., 2008; Gentile et al., 2011). The effect of litter quality

748 on SOC stabilization is mostly modulated by the extent of soil C saturation, and it

749 may alter SOC stocks only when there is a saturation deficit (Castellano et al., 2015).

750 Consistent with our results (Fig 7), previous studies also reported that litter quantity

751 rather than quality is one of the main determinants of SOC stability (Carrington et al.,

752 2012; Dungait et al., 2012). Experiments by Wang et al. (2016) suggested that the

753 ratio between different SOC fractions is related to microbial biomass and community

754 composition (which depends on the amounts of litter inputs), but not to litter chemical

755 composition.

756

757 **4.2 | Uncertainties in this study**

758 Some uncertainties in our simulation results may be caused by biases of forcing

759 and validation data. In this study, we assumed the forest and soil C at all observation

760 sites are at equilibrium. However, even though most observation sites have a stand

761 age older than 40 years and have not been strongly disturbed by fire or human

762 activities (e.g. reforestation and deforestation can induce a 30% change in soil C stock,

763 Don et al., 2011), the forest systems at some sites may not be at equilibrium,

764 especially under the background of global climate change. Some uncertainties also

765 arise due to lack of observations. Specifically, the wood and root litterfall at European

766 sites have not been measured and Chinese observation data only provides

767   measurements of plant biomass but not litterfall, so we have adopted the leaf turnover

768   rates and ratios of wood litter and root litter to leaf litter from databases of plant traits

769   and litterfall production to calculate the total litterfall production at each observation

770   site (see section 2.1). Moreover, most of the litter C:N ratios and the lignin:C ratios

771   were obtained from previously compiled litterfall databases and publications and not

772   from site level observations, Thus, biases and uncertainties that exist in the litter input

773   data are poorly quantified.

774   Additional uncertainties are related to model structural assumptions and

775   parameterizations. Specifically, soil moisture has been widely regarded as one of the

776   primary physical factors that control microbial activity (Arnold et al., 2015; Manzoni

777   et al., 2016; Ghezzehei et al., 2019); however the soil moisture control over microbial

778   dynamics is not used in the current parameterization of MIMICS. Soil structure

779   (characterized by porosity or bulk density) determines soil O_2 availability and the

780   accessibility of C particles to microbes (Lützow et al., 2006; Davidson et al., 2012).

781   Soil nutrient availability (e.g. mineral nitrogen and phosphorus) strongly affects

782   microbial C use efficiency and growth rate (Manzoni *et al*., 2017). Again, soil

783   moisture, structure and nutrient availability have not been considered in this

784   implement MIMICS. Finally, neither of the models considered here implement

785   vertically resolved soil biogeochemistry, which are clearly important to capture soils

786   with strong vertical profiles or vertical perturbations such as in permafrost C (Kovenet

787   al. 2015; McGuire et al. 2018). The insufficient representation of interactions between

788   soil physicochemical properties, nutrient availability, microbial dynamics and SOC

789   stabilization therefore may induce additional uncertainties in our results. We

790   appreciate that these additional complexities in model form also generates greater data

791   demands to appropriately parameterize and evaluate models, but may be necessary to

792   build confidence in soil carbon projections (Bradford *et al*. 2016).

793   **4.3 | Outlooks and challenges**

794   A study by Wieder et al. (2014) demonstrated that MIMICS could capture the

795   observed temporal decreasing trends of litter and SOC stocks in field decomposition

796   experiments. Our evaluation further demonstrates that MIMICS can simulate SOC

797 stock and composition across ecosystems with different climate, and soil and forest

798 types. MIMICS also represents the SOC decomposition and stabilization processes

799 more realistically (e.g. explicitly represents microbial dynamics) than conventional

800 first-order models. Therefore MIMICS can be used to replace the conventional

801 decomposition models used in existing ESMs.

802 The parameters, structure and algorithms of MIMICS can still be improved. We

803 encourage future studies to assess the global applicability of MIMICS or similar

804 models based on more integrated *in situ* observations on plant biomass, litterfall (both

805 aboveground and belowground), SOC stock and composition, soil physicochemical

806 properties and local climate from more ecosystems, in particular observations from

807 grasslands and tropical forests. We also encourage more studies to quantify the

808 interactions between soil physicochemical properties, microbial dynamics and the

809 stabilization of SOC. In this study, the MIMICS model considering the

810 physicochemical constraints of soil properties on SOC deprotection rate and microbe

811 turnover more accurately estimated SOC concentration than the default model (Fig. 2).

812 But the empirical functions (Eqs. 13, 14) used to represent physicochemical

813 constraints were built empirically based on analysis of the biases of simulated SOC

814 concentration from the default version of MIMICS (Fig. 3). More experiments

815 investigating influences of soil physicochemical properties on microbial activity and

816 the C adsorption/desorption rate of mineral soil are needed to improve these empirical

817 functions. Furthermore, many soil properties are significantly correlated (e.g. Fig. S12)

818 and the changes in litter inputs and SOC contents can in return dramatically alter soil

819 physical, chemical, and biological properties (Schmidt et al., 2011; Murphy et al.,

820 2015). Thus, research focusing on the interactions between litter, SOC and different

821 soil properties is also essential.

822

827 –FNRS. YPW acknowledge the financial support by the National Environmental

828 Science Program Earth System and Climate Change. WRW is supported by the US

829 Department of Energy under award number BSS DE-SC0016364, US Department of

830 Agriculture NIFA 2015-67003-23485, and NASA Interdisciplinary Science Program

831 award number NNX17AK19G. We acknowledge the contribution of Shijie Han,

832 Sheng Du, Shenggong Li, Keping Ma, Junhua Yan, Youxin Ma and Genxu Wang

833 from the Chinese Academy of Sciences to collecting the Chinese observation data.

834 We also acknowledge the collection of data by partners of the official UNECE ICP

835 Forests Network (http://icp-forests.net/contributors). Part of the data was co-financed

836 by the European Commission (Data achieved at 23/04/2018).

837

838 **Data accessibility**: The European ICP forest data can always be requested from the

839 Programme Co-ordinating Centre (PCC, http://icp-forests.net/page/data-requests) of

840 ICP Forests in Eberswalde, Germany. The Chinese forest data can be obtained by

841 contacting the Prof. Tang X (xltang@scib.ac.cn) in South China Botanical Garden,

842 Chinese Academy of Sciences, Guangzhou, China. All of the other databases of soil,

843 climate, litterfall and vegetation are publicly accessible, and the specific references

844 and links to these databases are provided in section 2.1.

845

846 **REFERENCES**

847 Abramoff, R., Xu, X., Hartman, M., O'Brien, S., Feng, W., Davidson, E., Finzi, A., Moorhead, D., Schimel, J.,

848 Torn, M. & Mayes, M.A. (2018). The Millennial model: in search of measurable pools and

849 transformations for modeling soil carbon in the new century. *Biogeochemistry*, 137, 51-71.

850 Abramoff, R. Z., Torn, M. S., Georgiou, K., Tang, J. & Riley, W. J. (2019). Soil organic matter temperature

851 sensitivity cannot be directly inferred from spatial gradients. *Global Biogeochemical Cycles*.

852 doi:10.1029/2018gb006001

853 Akaike, H. (1974). A new look at the statistical model identification, IEEE T. on Automat. Cont., 19, 716–723.

854 Allison, S. D. (2012). A trait-based approach for modelling microbial litter decomposition. *Ecology Letters*, 15,

855 1058-1070.

856 Allison, S. D., Wallenstein, M. D. & Bradford, M. A. (2010). Soil-carbon response to warming dependent on

857   microbial physiology. *Nature Geoscience*, 3, 336-340.

858   Arnold, C., Ghezzehei, T. A. & Berhe, A. A. (2015). Decomposition of distinct organic matter pools is regulated

859   by moisture status in structured wetland soils. *Soil Biology and Biochemistry*, 81, 28-37.

860   Bailey, V. L., Bond-Lamberty, B., De Angelis, K., Grandy, A. S., Hawkes, C. V., Heckman, K., . . . Wallenstein,

861   M. D. (2018). Soil carbon cycling proxies: Understanding their critical role in predicting climate change

862   feedbacks. *Global Chang Biology*, 24, 895-905.

863   Barré, P., Eglin, T., Christensen, B. T., Ciais, P., Houot, S., Kätterer, T., van Oort, F., Peylin, P., Poulton, P. R.,

864   Romanenkov, V. & Chenu, C. (2010). Quantifying and isolating stable soil organic carbon using

865   long-term bare fallow experiments. *Biogeosciences*, 7, 3839-3850.

866   Benbi, D. K., Boparai, A. K. & Brar, K. (2014). Decomposition of particulate organic matter is more sensitive to

867   temperature than the mineral associated organic matter. *Soil Biology and Biochemistry*, 70, 183-192.

868   Bonan, G. B., Hartman, M. D., Parton, W. J. & Wieder, W. R. (2013). Evaluating litter decomposition in earth

869   system models with long-term litterbag experiments: an example using the Community Land Model

870   version 4 (CLM4). *Global Chang Biology*, 19, 957-974.

871   Bradford, M. A., Wieder, W. R., Bonan, G. B., Fierer, N., Raymond, P. A., & Crowther, T. W. (2016). Managing

872   uncertainty in soil carbon feedbacks to climate change. *Nature Climate Change, 6*, 751-758.

873   Campbell, E. E. & Paustian, K. (2015). Current developments in soil organic matter modeling and the expansion of

874   model applications: a review. *Environmental Research Letters*, 10, 123004.

875   Campbell, E. E., Parton, W. J., Soong, J. L., Paustian, K., Hobbs, N. T. & Cotrufo, M. F. (2016). Using litter

876   chemistry controls on microbial processes to partition litter carbon fluxes with the Litter Decomposition

877   and Leaching (LIDEL) model. *Soil Biology and Biochemistry*, 100, 160-174.

878   Carrington, E. M., Hernes, P. J., Dyda, R. Y., Plante, A. F. & Six, J. (2012). Biochemical changes across a carbon

879   saturation gradient: Lignin, cutin, and suberin decomposition and stabilization in fractionated carbon

880   pools. *Soil Biology and Biochemistry*, 47, 179-190.

881   Castellano, M. J., Mueller, K. E., Olk, D. C., Sawyer, J. E. & Six, J. (2015) Integrating plant litter quality, soil

882   organic matter stabilization, and the carbon saturation concept. *Global Chang Biology*, 21, 3200-3209.

883   Ciais, P., Sabine, C., Bala, G., Bopp, L., Brovkin, V., Canadell, J., Chhabra, A., DeFries, R., Galloway, J.,

884   Heimann, M., Jones, C., Le Quéré, C., Myneni, R. B., Piao, S. L. & Thornton, P. (2013). Carbon and

885   Other Biogeochemical Cycles. In: *Climate Change 2013: The Physical Science Basis. Contribution of*

886   *Working Group I to the Fifth Assessment Report of the Intergovernmental Panel on Climate Change* eds.

887   T. F. Stocker, D. Qin, G.-K. Plattner, M. Tignor, S. K. Allen, J. Boschung, A. Nauels, Y. Xia, V. Bex

888   and M. P.M.). Cambridge University Press, Cambridge, United Kingdom and New York, NY, USA.

889 Cools, N. & De Vos, B. (2016). Part X: Sampling and Analysis of Soil. In: UNECE ICP Forests Programme

890   Coordinating Centre (ed.): Manual on methods and criteria for harmonized sampling, assessment,

891   monitoring and analysis of the effects of air pollution on forests. In, Thünen Institute of Forest

892   Ecosystems, Eberswalde, Germany.

893 Cotrufo, M. F., Wallenstein, M. D., Boot, C. M., Denef, K. & Paul, E. (2013). The Microbial Efficiency-Matrix

894   Stabilization (MEMS) framework integrates plant litter decomposition with soil organic matter

895   stabilization: do labile plant inputs form stable soil organic matter? *Glob Chang Biol*, 19, 988-995.

896 Creamer, C. A., de Menezes, A. B., Krull, E. S., Sanderman, J., Newton-Walters, R. & Farrell, M. (2015).

897   Microbial community structure mediates response of soil C decomposition to litter addition and warming.

898   *Soil Biology and Biochemistry*, 80, 175-188.

899 Dai, Y., Shangguan, W., Wang, D., Wei, N., Xin, Q., Yuan, H., Zhang, S., Liu, S. & Yan, F. (2018) A review on

900   the global soil datasets for earth system modeling. *SOIL Discussions*, 1-30.

901 Davidson, E. A., Samanta, S., Caramori, S. S. & Savage, K. (2012). The Dual Arrhenius and Michaelis-Menten

902   kinetics model for decomposition of soil organic matter at hourly to seasonal time scales. *Global Change*

903   *Biology*, 18, 371-384.

904 Doetterl, S., Stevens, A., Six, J., Merckx, R., Van Oost, K., Casanova Pinto, M., Casanova-Katny, A., Muñoz, C.,

905   Boudin, M., Venegas, E. & Boeckx, P. (2015). Soil carbon storage controlled by interactions between

906   geochemistry and climate. *Nature Geoscience*, 8, 780–783.

907 Don, A., Schumacher, J. & Freibauer, A. (2011). Impact of tropical land-use change on soil organic carbon stocks

908   – a meta-analysis. *Global Change Biology*, 17, 1658-1670.

909 Duan, Q., Gupta, V. & Sorooshian, S. (1993). Shuffled complex evolution approach for effective and efficient

910   global minimization. *Journal of Optimization Theory and Its Applications*, 76, 501-521.

911 Duan, Q., Sorooshian, S. & Gupta, V. K. (1994). Optimal use of the SCE-UA global optimization method for

912   calibrating watershed models. *Journal of Hydrology*, 158, 265-284.

913 Dungait, J. A. J., Hopkins, D. W., Gregory, A. S. & Whitmore, A.P. (2012). Soil organic matter turnover is

914   governed by accessibility not recalcitrance. *Global Change Biology*, 18, 1781-1796.

915 Elliott, E. T., Paustian, K. & Frey, S. D. (1996). Modeling the Measurable or Measuring the Modelable: A

916   Hierarchical Approach to Isolating Meaningful Soil Organic Matter Fractionations. In: Powlson D. S.,

917   Smith P., Smith J. U. (eds) *Evaluation of Soil Organic Matter Models. NATO ASI Series* (*Series I:*

918   *Global Environmental Change*), vol 38. Springer, Berlin, Heidelberg.

919 FAO/IIASA/ISRIC/ISSCAS/JRC (2012). Harmonized World Soil Database (version 1.2). In, FAO, Rome, Italy

920   and IIASA, Laxenburg, Austria.

921 Fontaine, S., Barot, S., Barré, P., Bdioui, N., Mary, B. & Rumpel, C. (2007). Stability of organic carbon in deep

922   soil layers controlled by fresh carbon supply. *Nature*, 450, 277-280.

923 Frankenberg, C., Fisher, J. B., Worden, J., Badgley, G., Saatchi, S.S., Lee, J. E., Toon, G. C., Butz, A., Jung, M. &

924   Kuze, A. (2011). New global observations of the terrestrial carbon cycle from GOSAT: Patterns of plant

925   fluorescence with gross primary productivity. *Geophysical Research Letters*, 38, 351-365.

926 Gentile, R., Vanlauwe, B. & Six, J. (2011). Litter quality impacts short- but not long-term soil carbon dynamics in

927   soil aggregate fractions. *Ecological Applications*, 21, 695-703.

928 Georgiou, K., Abramoff, R. Z., Harte, J., Riley, W. J. & Torn, M. S. (2017). Microbial community-level regulation

929   explains soil carbon responses to long-term litter manipulations. *Nature Communications*, 8, 1223.

930 Ghezzehei, T. A., Sulman, B., Arnold, C. L., Bogie, N. A. & Berhe, A. A. (2019). On the role of soil water

931   retention characteristic on aerobic microbial respiration. *Biogeosciences*, 16, 1187-1209.

932 Hararuk, O. & Luo, Y. (2014). Improvement of global litter turnover rate predictions using a Bayesian MCMC

933   approach. *Ecosphere*, 5, art163.

934 Harmon, M. E., Silver, W. L., Fasth, B., Chen, H. U. A., Burke, I. C., Parton, W. J., Hart, S. C. & Currie, W. S.

935   (2009). Long-term patterns of mass loss during the decomposition of leaf and fine root litter: an intersite

936   comparison. *Global Change Biology*, 15, 1320-1338.

937 Hartono, A., Funakawa, S. & Kosaki, T. (2005). Phosphorus Sorption-Desorption Characteristics of Selected Acid

938   Upland Soils in Indonesia. *Soil Science and Plant Nutrition*, 51, 787-799.

939 Heimann, M. & Reichstein, M. (2008). Terrestrial ecosystem carbon dynamics and climate feedbacks. *Nature*, 451,

940   289-292.

941 Helfrich, M., Ludwig, B., Potthoff, M. & Flessa, H. (2008). Effect of litter quality and soil fungi on

942   macroaggregate dynamics and associated partitioning of litter carbon and nitrogen. *Soil Biology and*

943   *Biochemistry*, 40, 1823-1835.

944 Hibbing, M. E., Fuqua, C., Parsek, M. R. & Peterson, S. B. (2010) Bacterial competition: surviving and thriving in

945   the microbial jungle. *Nature Reviews Microbiology*, 8, 15-25.

946 Holland, E. A., Post, W. M., Matthews, E., Sulzman, J., Staufer, R. & Krankina, O. (2015). A Global Database of

947   Litterfall Mass and Litter Pool Carbon and Nutrients. Data set. Available on-line [http://daac.ornl.gov]

948   from Oak Ridge National Laboratory Distributed Active Archive Center. In, Oak Ridge, Tennessee,

949   USA.

950   Huang, Y., Guenet, B., Ciais, P., Janssens, I.A., Soong, J. L., Wang, Y., Goll, D., Blagodatskaya, E. & Huang, Y.

951   (2018). ORCHIMIC (v1.0), A microbe-driven model for soil organic matter decomposition designed for

952   large-scale applications. *Geoscientific Model Development*, 11, 2111-2138.

953   Iversen, C. M., McCormack, M. L., Powell, A. S., Blackwood, C. B., Freschet, G. T., Kattge, J., Roumet, C.,

954   Stover, D. B., Soudzilovskaia, N. A., Valverde-Barrantes, O. J., van Bodegom, P. M. & Violle, C. (2017).

955   A global Fine-Root Ecology Database to address below-ground challenges in plant ecology. *New*

956   *Phytologist*, 215, 15-26.

957   Jenkinson, D. & Rayner, J. (1977). The turnover of soil organic matter in some of the Rothamsted classical

958   experiments. *Soil Science*, 123, 298-305.

959   Jia, B., Zhou, G. & Xu, Z. (2016). Forest litterfall and its composition: a new data set of observational data from

960   China. *Ecology*, 97, 1365.

961   Jobbágy, E. G. & Jackson, R. B. (2000). The Vertical Distribution of Soil Organic Carbon and Its Relation to

962   Climate and Vegetation. *Ecological Applications*, 10, 423-436.

963   Jung, M., Reichstein, M., Ciais, P., Seneviratne, S.I., Sheffield, J., Goulden, M. L., Bonan, G., Cescatti, A., Chen,

964   J., de Jeu, R., Dolman, A. J., Eugster, W., Gerten, D., Gianelle, D., Gobron, N., Heinke, J., Kimball, J.,

965   Law, B. E., Montagnani, L., Mu, Q., Mueller, B., Oleson, K., Papale, D., Richardson, A. D., Roupsard,

966   O., Running, S., Tomelleri, E., Viovy, N., Weber, U., Williams, C., Wood, E., Zaehle, S. & Zhang, K.

967   (2010). Recent decline in the global land evapotranspiration trend due to limited moisture supply. *Nature*,

968   467, 951-954.

969   Kaiser, C., Franklin, O., Dieckmann, U. & Richter, A. (2014). Microbial community dynamics alleviate

970   stoichiometric constraints during litter decay. *Ecology Letters*, 17, 680-690.

971   Kaiser, C., Franklin, O., Richter, A. & Dieckmann, U. (2015). Social dynamics within decomposer communities

972   lead to nitrogen retention and organic matter build-up in soils. *Nat Commun*, 6, 8960.

973   Kallenbach, C., Frey, S. & Grandy, S. (2016). Direct evidence for microbial-derived soil organic matter formation

974   and its ecophysiological controls. *Nature Communications*, 7, 13630.

975   Kattge, J., *et al*. (2011). TRY - a global database of plant traits. *Global Change Biology*, 17, 2905-2935.

976   Kothawala, D. N., Moore, T. R. & Hendershot, W. H. (2008). Adsorption of dissolved organic carbon to mineral

977   soils: A comparison of four isotherm approaches. *Geoderma*, 148, 43-50.

978   Koven, C. D., Lawrence, D. M., & Riley, W. J. (2015). Permafrost carbon−climate feedback is sensitive to deep

979   soil carbon decomposability but not deep soil nitrogen dynamics. *Proceedings of the National Academy*

980   *of Sciences*, 112, 3752-3757.

981   Koven, C. D., Riley, W. J., Subin, Z. M., Tang, J. Y., Torn, M. S. Collins, W. D., Bonan, G. B., Lawrence, D. M.

982   & Swenson, S. C. (2013). The effect of vertically resolved soil biogeochemistry and alternate soil C and

983   N models on C dynamics of CLM4. *Biogeosciences*, 10, 7109-7131.

984   Krinner, G., Viovy, N., de Noblet-Ducoudré, N., Ogée, J., Polcher, J., Friedlingstein, P., Ciais, P., Sitch, S. &

985   Prentice, I.C. (2005). A dynamic global vegetation model for studies of the coupled

986   atmosphere-biosphere system. *Global Biogeochemical Cycles*, 19

987   Kuzyakov, Y. (2010). Priming effects: Interactions between living and dead organic matter. *Soil Biology and*

988   *Biochemistry*, 42, 1363-1371.

989   Lützow, M. v., Kögel-Knabner, I., Ekschmitt, K., Flessa, H., Guggenberger, G., Matzner, E. & Marschner, B.

990   (2007). SOM fractionation methods: Relevance to functional pools and to stabilization mechanisms. *Soil*

991   *Biology and Biochemistry*, 39, 2183-2207.

992   Lützow, M. v., Kogel-Knabner, I., Ekschmitt, K., Matzner, E., Guggenberger, G., Marschner, B. & Flessa, H.

993   (2006). Stabilization of organic matter in temperate soils: mechanisms and their relevance under

994   different soil conditions - a review. *European Journal of Soil Science*, 57, 426-445.

995   Lal, R. (2016). Beyond COP 21: Potential and challenges of the "4 per Thousand" initiative. *Journal of Soil and*

996   *Water Conservation*, 71, 20A-25A.

997   Lehmann, J. & Kleber, M. (2015). The contentious nature of soil organic matter. *Nature*, 528, 60-68.

998   Liang, S., Zhao, X., Liu, S., Yuan, W., Cheng, X., Xiao, Z., Zhang, X., Liu, Q., Cheng, J., Tang, H., Qu, Y., Bo, Y.,

999   Qu, Y., Ren, H., Yu, K. & Townshend, J. (2013). A long-term Global LAnd Surface Satellite (GLASS)

1000   data-set for environmental studies. *International Journal of Digital Earth*, 6, 5-33.

1001   Manzoni, S. & Porporato, A. (2009). Soil carbon and nitrogen mineralization: Theory and models across scales.

1002   *Soil Biology and Biochemistry*, 41, 1355-1379.

1003   Manzoni, S., Moyano, F., Kätterer, T. & Schimel, J. (2016). Modeling coupled enzymatic and solute transport

1004   controls on decomposition in drying soils. *Soil Biology and Biochemistry*, 95, 275-287.

1005   Manzoni, S., Taylor, P., Richter, A., Porporato, A. & Agren, G. I. (2012). Environmental and stoichiometric

1006   controls on microbial carbon-use efficiency in soils. *New Phytologist*, 196, 79-91.

1007   Manzoni, S., Capek, P., Mooshammer, M., Lindahl, B. D., Richter, A. & Santruckova, H. (2017). Optimal

1008   metabolic regulation along resource stoichiometry gradients. *Ecol Lett*, 20, 1182-1191.

1009   McGuire, A. D., Lawrence, D. M., Koven, C., Clein, J. S., Burke, E., Chen, G. & Zhuang, Q. (2018). Dependence

1010   of the evolution of carbon dynamics in the northern permafrost region on the trajectory of climate

1011   change. *Proceedings of the National Academy of Sciences*. 115, 3882-3887.

1012   Muttil, N. & Jayawardena, A. W. (2008). Shuffled Complex Evolution model calibrating algorithm: enhancing its

1013   robustness and efficiency. *Hydrological Processes*, 22, 4628-4638.

1014   Parton, W., Silver, W. L., Burke, I. C., Grassens, L., Harmon, M. E., Currie, W. S., King, J. Y., Adair, E. C.,

1015   Brandt, L.A., Hart, S. C. & Fasth, B. (2007). Global-scale similarities in nitrogen release patterns during

1016   long-term decomposition. *Science*, 315, 361-364.

1017   Parton, W. J., Schimel, D. S., Cole, C. V. & Ojima, D. S. (1987). Analysis of Factors Controlling Soil Organic

1018   Matter Levels in Great Plains Grasslands1. *Soil Science Society of America Journal*, 51, 1173-1179.

1019   Rasmussen, C., Heckman, K., Wieder, W. R., Keiluweit, M., Lawrence, C. R., Berhe, A. A., Blankinship, J. C.,

1020   Crow, S. E., Druhan, J. L., Hicks Pries, C. E., Marin-Spiotta, E., Plante, A.F., Schädel, C., Schimel, J. P.,

1021   Sierra, C. A., Thompson, A. & Wagai, R. (2018). Beyond clay: towards an improved set of variables for

1022   predicting soil organic matter content. *Biogeochemistry*, 137, 297-306.

1023   Robertson, A. D., Paustian, K., Ogle, S., Wallenstein, M. D., Lugato, E. & Cotrufo, M. F. (2019). Unifying soil

1024   organic matter formation and persistence frameworks: the MEMS model. *Biogeosciences*, 16,

1025   1225-1248.

1026   Schimel, D. S., Braswell, B. H., Holland, E. A., McKeown, R., Ojima, D. S., Painter, T. H., Parton, W. J. &

1027   Townsend, A. R. (1994). Climatic, edaphic, and biotic controls over storage and turnover of carbon in

1028   soils. *Global Biogeochemical Cycles*, 8, 279-293.

1029   Schimel, J. P. & Weintraub, M. N. (2003). The implications of exoenzyme activity on microbial carbon and

1030   nitrogen limitation in soil: a theoretical model. *Soil Biology and Biochemistry*, 35, 549-563.

1031   Schmidt, M. W., Torn, M. S., Abiven, S., Dittmar, T., Guggenberger, G., Janssens, I. A., Kleber, M.,

1032   Kogel-Knabner, I., Lehmann, J., Manning, D. A., Nannipieri, P., Rasse, D. P., Weiner, S. & Trumbore,

1033   S.E. (2011) Persistence of soil organic matter as an ecosystem property. *Nature*, 478, 49-56.

1034   Shangguan, W., Dai, Y., Duan, Q., Liu, B. & Yuan, H. (2014). A global soil data set for earth system modeling.

1035   *Journal of Advances in Modeling Earth Systems*, 6, 249-263.

1036   Shi, Z., Crowell, S., Luo, Y. & Moore, B., III. (2018). Model structures amplify uncertainty in predicted soil

1037   carbon responses to climate change. *Nature Communications*, 9, 2171.

1038   Sierra, C. A., Trumbore, S. E., Davidson, E. A., Vicca, S. & Janssens, I. (2015). Sensitivity of decomposition rates

1039   of soil organic matter with respect to simultaneous changes in temperature and moisture. *Journal of*

1040   *Advances in Modeling Earth Systems*, 7, 335-356.

1041   Six, J., Bossuyt, H., Degryze, S. & Denef, K. (2004). A history of research on the link between (micro)aggregates,

1042   soil biota, and soil organic matter dynamics. *Soil and Tillage Research*, 79, 7-31.

1043   Six, J., Feller, C., Denef, K., Ogle, S.M., de Moraes, J.C. & Albrecht, A. (2002). Soil organic matter, biota and

1044   aggregation in temperate and tropical soils - Effects of no-tillage. *Agronomie*, 22, 755-775.

1045   Six, J. & Paustian, K. (2014) Aggregate-associated soil organic matter as an ecosystem property and a

1046   measurement tool. *Soil Biology & Biochemistry*, 68, A4-A9.

1047   Sitch, S., Smith, B., Prentice, I. C., Arneth, A., Bondeau, A., Cramer, W., Kaplan, J. O., Levis, S., Lucht, W.,

1048   Sykes, M. T., Thonicke, K., & Venevsky, S. (2003) Evaluation of ecosystem dynamics, plant geography

1049   and terrestrial carbon cycling in the LPJ dynamic global vegetation model, *Global Change Biology*, 9,

1050   161–185.

1051   Sokol, N. W., Sanderman, J. & Bradford, M. A. (2019). Pathways of mineral-associated soil organic matter

1052   formation: Integrating the role of plant carbon source, chemistry, and point of entry. *Global Change*

1053   *Biology*, 25, 12-24.

1054   Stewart, C. E., Paustian, K., Conant, R. T., Plante, A. F. & Six, J. (2007). Soil carbon saturation: concept, evidence

1055   and evaluation. *Biogeochemistry*, 86, 19-31.

1056   Stewart, C. E., Plante, A. F., Paustian, K., Conant, R. T. & Six, J. (2008). Soil Carbon Saturation: Linking Concept

1057   and Measurable Carbon Pools. *Soil Science Society of America Journal*, 72, 379.

1058   Stockmann, U., Adams, M. A., Crawford, J. W., Field, D. J., Henakaarchchi, N., Jenkins, M., Minasny, B.,

1059   McBratney, A. B., Courcelles, V. d. R. d., Singh, K., Wheeler, I., Abbott, L., Angers, D. A., Baldock, J.,

1060   Bird, M., Brookes, P. C., Chenu, C., Jastrow, J. D., Lal, R., Lehmann, J., O'Donnell, A. G., Parton, W. J.,

1061   Whitehead, D. & Zimmermann, M. (2013). The knowns, known unknowns and unknowns of

1062   sequestration of soil organic carbon. *Agriculture, Ecosystems & Environment*, 164, 80-99.

1063   Tang, J. & Zhuang, Q. (2013). A global sensitivity analysis and Bayesian inference framework for improving the

1064   parameter estimation and prediction of a process-based Terrestrial Ecosystem Mode. *Journal of*

1065   *Geophysical Research:Atmospheres*, D15303. doi:10.1029/2009JD011724

1066   Tang, X., Zhao, X., Bai, Y., Tang, Z., Wang, W., Zhao, Y., Wan, H., Xie, Z., Shi, X., Wu, B., Wang, G., Yan, J.,

1067   Ma, K., Du, S., Li, S., Han, S., Ma, Y., Hu, H., He, N., Yang, Y., Han, W., He, H., Yu, G., Fang, J. &

1068   Zhou, G. (2018). Carbon pools in China's terrestrial ecosystems: New estimates based on an intensive

1069   field survey. *Proc Natl Acad Sci U S A*, 115, 4021-4026.

1070   Tarnocai, C., Canadell, J. G., Schuur, E. A. G., Kuhry, P., Mazhitova, G. & Zimov, S. (2009). Soil organic carbon

1071   pools in the northern circumpolar permafrost region. *Global Biogeochemical Cycles*, 23, GB2023,

1072   doi:10.1029/2008GB003327

1073   Thornton, P. E. & Rosenbloom, N. A. (2005). Ecosystem model spin-up: Estimating steady state conditions in a

1074   coupled terrestrial carbon and nitrogen cycle model. *Ecological Modelling*, 189, 25-48.

1075   Tifafi, M., Guenet, B. & Hatté C. (2018). Large Differences in Global and Regional Total Soil Carbon Stock

1076   Estimates Based on SoilGrids, HWSD, and NCSCD: Intercomparison and Evaluation Based on Field

1077   Data From USA, England, Wales, and France. *Global Biogeochemical Cycles*, 32, 42-56.

1078   Todd-Brown, K. E. O., Randerson, J. T., Post, W. M., Hoffman, F. M., Tarnocai, C., Schuur, E. A. G. & Allison, S.

1079   D. (2013). Causes of variation in soil carbon simulations from CMIP5 Earth system models and

1080   comparison with observations. *Biogeosciences*, 10, 1717-1736.

1081   Tucker, C. J., Pinzon, J. E., Brown, M. E., Slayback, D. A., Pak, E. W., Mahoney, R., Vermote, E. F. & El Saleous,

1082   N. (2005). An extended AVHRR 8-km NDVI dataset compatible with MODIS and SPOT vegetation

1083   NDVI data. *International Journal of Remote Sensing*, 26, 4485-4498.

1084   Ukonmaanaho, L., Pitman, R., Bastrup-Birk, A., Breda, N. & Rautio, P. (2016). Part XIII: Sampling and Analysis

1085   of Litterfall. In: UNECE ICP Forests Programme Co-ordinating Centre (ed.): Manual on methods and

1086   criteria for harmonized sampling, assessment, monitoring and analysis of the effects of air pollution on

1087   forests. In, Thünen Institute for Forests Ecosystems, Eberswalde, Germany.

1088   Viovy, N. (2018). CRUNCEP Version 7 - Atmospheric Forcing Data for the Community Land Model. Research

1089   Data Archive at the National Center for Atmospheric Research,. In, Computational and Information

1090   Systems Laboratory. http://rda.ucar.edu/datasets/ds314.3/.

1091   Viscarra Rossel, R. A. & Hicks, W. S. (2015). Soil organic carbon and its fractions estimated by visible-near

1092   infrared transfer functions. *European Journal of Soil Science*, 66, 438-450.

1093   Viscarra Rossel, R. A., Lee, J., Berhrens, T., Luo, Z., Baldock, J. & Richards, A. (2019). Continental-scale soil

1094   carbon composition and vulnerability modulated by regional environmental controls. *Nature Geoscience*,

1095   12, 547-552.

1096   Wagner, S., Cattle, S. R. & Scholten, T. (2007). Soil-aggregate formation as influenced by clay content and

1097   organic-matter amendment. *Journal of Plant Nutrition and Soil Science*, 170, 173-180.

1098   Wang, G., Post, W. M. & Mayes, M. A. (2013). Development of microbial-enzyme-mediated decomposition

1099   model parameters through steady-state and dynamic analyses. *Ecological Applications*, 23, 255-272.

1100   Wang, Q., He, T. & Liu, J. (2016). Litter input decreased the response of soil organic matter decomposition to

1101   warming in two subtropical forest soils. *Scitific Reports*, 6, 33814.

1102   Wang, Y. P., Chen, B.C., Wieder, W. R., Leite, M., Medlyn, B. E., Rasmussen, M., Smith, M. J., Agusto, F. B.,

1103   Hoffman, F. & Luo, Y. Q. (2014). Oscillatory behavior of two nonlinear microbial models of soil carbon

1104   decomposition. *Biogeosciences*, 11, 1817-1831.

1105   Wieder, W. R., Bonan, G. B. & Allison, S.D. (2013). Global soil carbon projections are improved by modelling

1106   microbial processes. *Nature Climate Change*, 3, 909-912.

1107   Wieder, W. R., Boehnert, J. & Bonan, G. B. (2014a). Evaluating soil biogeochemistry parameterizations in Earth

1108   system models with observations. *Global Biogeochemical Cycles*, 28, 211-222.

1109   Wieder, W. R., Grandy, A. S., Kallenbach, C. M. & Bonan, G. B. (2014b). Integrating microbial physiology and

1110   physio-chemical principles in soils with the MIcrobial-MIneral Carbon Stabilization (MIMICS) model.

1111   *Biogeosciences*, 11, 3899-3917.

1112   Wieder, W. R., Grandy, A. S., Kallenbach, C. M., Taylor, P. G. & Bonan, G. B. (2015). Representing life in the

1113   Earth system with soil microbial functional traits in the MIMICS model. *Geoscientific Model*

1114   *Development*, 8, 1789-1808.

1115   Wieder, W. R., Hartman, M. D., Sulman, B. N., Wang, Y-P, Koven, C. D. & Bonan, G. B. (2018). Carbon cycle

1116   confidence and uncertainty: Exploring variation among soil biogeochemical models. *Global Change*

1117   *Biology.*, 24, 1563–1579.

1118   Wu, D., Piao, S., Liu, Y., Ciais, P. & Yao, Y. (2018). Evaluation of CMIP5 Earth System Models for the Spatial

1119   Patterns of Biomass and Soil Carbon Turnover Times and Their Linkage with Climate. *Journal of*

1120   *Climate*, 31, 5947-5960.

1121   Xia, J. Y., Luo, Y. Q., Wang, Y. P., Weng, E. S. & Hararuk, O. (2012). A semi-analytical solution to accelerate

1122   spin-up of a coupled carbon and nitrogen land model to steady state. *Geoscientific Model Development*,

1123   5, 1259-1271.

1124   Xu, X., Thornton, P. E. & Post, W. M. (2013). A global analysis of soil microbial biomass carbon, nitrogen and

1125   phosphorus in terrestrial ecosystems. *Global Ecology and Biogeography*, 22, 737-749.

1126   Zhang, H., Yuan, W., Dong, W. & Liu, S. (2014). Seasonal patterns of litterfall in forest ecosystem worldwide.

1127   *Ecological Complexity*, 20, 240-247.

1128 Zhang, H., Goll, D. S., Manzoni, S., Ciais, P., Guenet, B. & Huang, Y. (2018). Modeling the effects of litter

1129   stoichiometry and soil mineral N availability on soil organic matter formation using CENTURY-CUE

1130   (v1.0). *Geoscientific Model Development*, 11, 4779-4796.

1131

1132 **Table**

1133

1134 **Table 1** Tested models in this study and parameters subject to optimization of each

1135 model. k_{litt} and k_{soc} tune the turnover rate of litter and SOC pools in CENTURY,

1136 respectively. a_v and a_k are parameters tune microbial maximum reaction velocity (Eq.

1137 4) and half-saturation constant (Eq. 5). k_d, k_{dp} and k_{bs} tune the deprotection rate of

1138 SOC_p (Eqs. 13-15). β tunes the density-dependent microbial turnover rate (Eq. 16).

Model	Optimized parameters
CENTURY	k_{litt}, k_{soc}
MIMICS-def	a_v, a_k, k_d
MIMICS-D	a_v, a_k, k_d, k_{dp}
MIMICS-DB	a_v, a_k, k_d, k_{dp}, k_{bs}
MIMICS-DBT	a_v, a_k, k_d, k_{dp}, k_{bs}, β

1139

1140

1141 **Figure**

1142 **Figure 1** Soil C pools and fluxes represented in CENTURY (a) and MIMICS (b). In

1143 both models, litter inputs (Lit_{inp}) are partitioned into metabolic and structural litter

1144 pools (LIT_m and LIT_s) based on litter quality (f_{met}). The soil organic carbon (SOC) in

1145 CENTURY are divided into active (SOC_{act}), slow (SOC_{slow}) and passive (SOC_{pas})

1146 pools. CUE is the carbon use efficiency of decomposed litter or SOC. In MIMICS,

1147 decomposition of litter and available SOM pools (SOC_a) are governed by temperature

1148 sensitive Michaelis–Menten kinetics (V_{max} and K_m). Microbial growth efficiency

1149 (MGE) determines the partitioning of C fluxes entering microbial biomass pools vs.

1150   heterotrophic respiration. Turnover of the microbial biomass (τ) depends on microbial

1151   functional type (MIC_r and MIC_k), and is partitioned into available, physically and

1152   physicochemically protected, and chemically recalcitrant SOC pools (SOC_a, SOC_p,

1153   and SOC_c, respectively). $f_{i,met}$ and $f_{i,stru}$ denote the fraction of decomposed metabolic

1154   litter to SOC_p and the fraction of decomposed structural litter to SOC_c, respectively. f_p

1155   and f_c denote the fraction of τ partitioned to SOC_p and the fraction of τ partitioned to

1156 SOC_c, respectively.

1157

1158   **Figure 2** Comparison of CENTURY (a) and MIMICS (b-e) for simulating large-scale

1159   variation of SOC concentrations across the 206 forest sites in Europe and China.

1160   RMSE is the root mean square error, and AIC is the Akaike information criterion.

1161   MIMICS versions include the default model (MIMICS-def), revised SOC

1162   deprotection rate (MIMICS-D), using base saturation to modify deprotection rates

1163   (MIMICS-DB); and density-dependent microbial turnover rate (MIMICS-DBT; see

1164   section 2.2.2).

1165

1166   **Figure 3** Partial correlation coefficients between the biases of simulated SOC

1167   concentrations and the climate condition, amount and quality of litter input, and soil

1168   physical and chemical properties. MAT: mean annual temperature (°C), MAP: mean

1169   annual total precipitation (mm), MAP-PET: the difference between annual total

1170   precipitation and potential evapotranspiration (mm), ET: evapotranspiration (mm),

1171 LAI_{max}: mean of the annual maximum leaf area index at the observation site during

1172   the period from 1982 to 2000, LAI_{trend}: change trend of the LAI_{max} during the period

1173   from 1982 to 2000 (yr^{-1}), $NDVI_{max}$: mean of the annual maximum normalized

1174   difference vegetation index at the observation site during the period from 1982 to

1175   2000, LAI_{trend}: change trend of the $NDVI_{max}$ during the period from 1982 to 2000

1176   (yr^{-1}), $litter_{ab}$: aboveground litter-C stock (g C m^{-2}), SWC: soil water content, BD:

1177   bulk density (g cm^{-3}), BS: base saturation (0-1, dimensionless), CEC: Cation of

1178   exchange capacity (cmol kg^{-1}). Partial correlation coefficients between -0.14 and 0.14

1179   were not significant (p > 0.05).

1180

1181   **Figure 4** Sensitivity of simulated SOC concentration to mean annual temperature

1182   (S_{MAT}, a), soil water content (S_{SWC}, b), soil clay fraction (S_{clay}, c), annual litterfall

1183   input ($S_{litterfall}$, d), the C:N ratio of litterfall ($S_{C:N}$, e) and the lignin:C ratio of litterfall

1184   ($S_{lignin:C}$, f). The blue and red dashed lines denote insignificant and significant ($p<0.05$)

1185   sensitivity calculated based on observation data, respectively. The solid line in each

1186   box denotes the median value. Box boundaries show the 25th and 75th percentiles,

1187   whiskers denote the 10th and 90th percentiles, and the black dots denote the 5th and

1188   95th percentiles.

1189

1190   **Figure 5** Comparison between the simulated ratio of microbial C (MIC) to total SOC

1191   from different versions of MIMICS and the observed values at globally-distributed

1192   forest sites. The dashed and solid lines in each box are the mean and median value,

1193   respectively. Box boundaries show the 25th and 75th percentiles, whiskers denote the

1194   10th and 90th percentiles, the dots below and above each box denote the 5th and 95th

1195   percentiles, respectively. The 655 samples of observed MIC/SOC at

1196   globally-distributed forest sites are collected by Xu et al., 2013.

1197

1198   **Figure 6** Comparison between the simulated SOC compositions from optimized

1199   MIMICS (a) and CENTURY (b) model and the observed SOC compositions at 505

1200   sites in Australia (c). The observation data in Australia are obtained from

1201   Viscarra-Rossel et al. (2019). Viscarra-Rossel et al. partitioned total SOC into three

1202   fractions with different particle-sizes: the particulate organic carbon (POC), the humic

1203   organic carbon (HOC) and the resistant organic carbon (ROC, which is the

1204   mineral-associated organic carbon). The line in each box denotes median value. Box

1205   boundaries show the 25th and 75th percentiles, whiskers denote the 10th and 90th

1206   percentiles, and the dots below and above each box denote the 5th and 95th percentiles.

1207

1208   **Figure 7** Partial correlation coefficients between fraction of each SOC pool and

1209   model drivers, including mean annual temperature (MAT, °C), soil water content

1210   (SWC, dimensionless), soil clay content (clay, dimensionless), annual total litterfall

1211   production (Litterfall, g C m^{-2} yr^{-1}), litter C:N ratio (C:N), litter lignin:C ratio

1212   (Lignin:C), base saturation (BS, 0-1, dimensionless) and total SOC concentration

1213   (SOC), Figure (a) Obs show the results based on observation data from Australia.

1214   Figure (b)-(f) showed the results based on optimized CENTURY and MIMICS

1215   models. Partial correlation coefficients between -0.14 and 0.14 were not significant

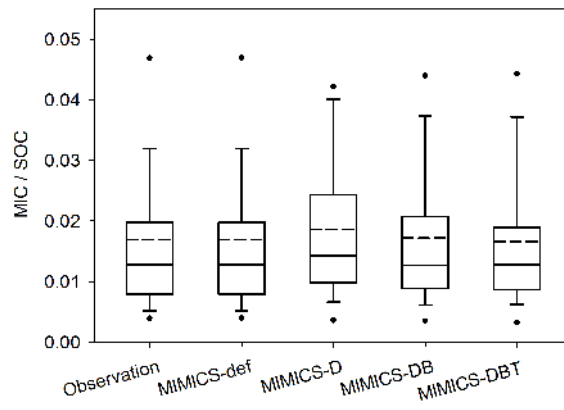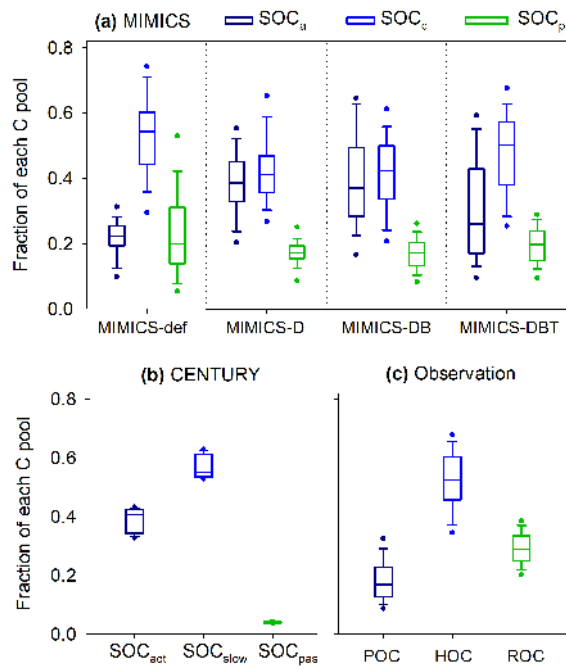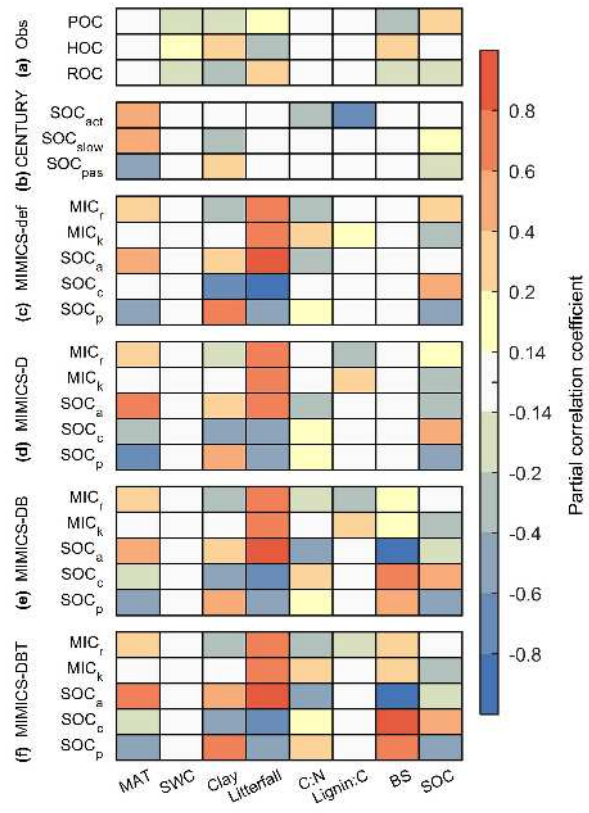1216   (p > 0.05).
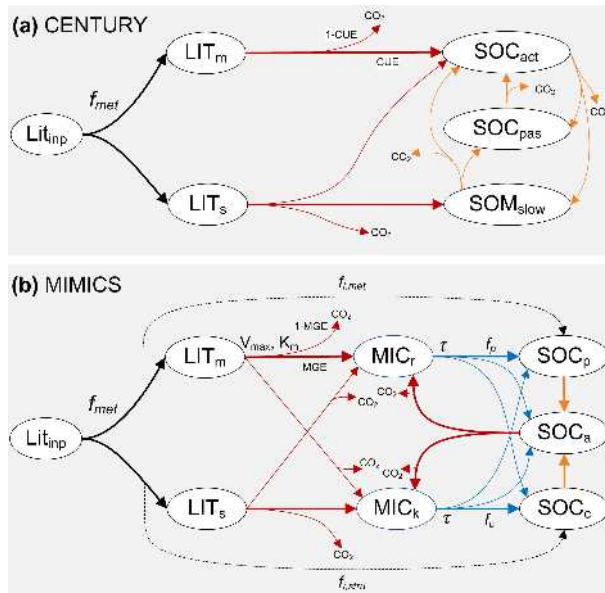
gcb_14994_f1.jpg
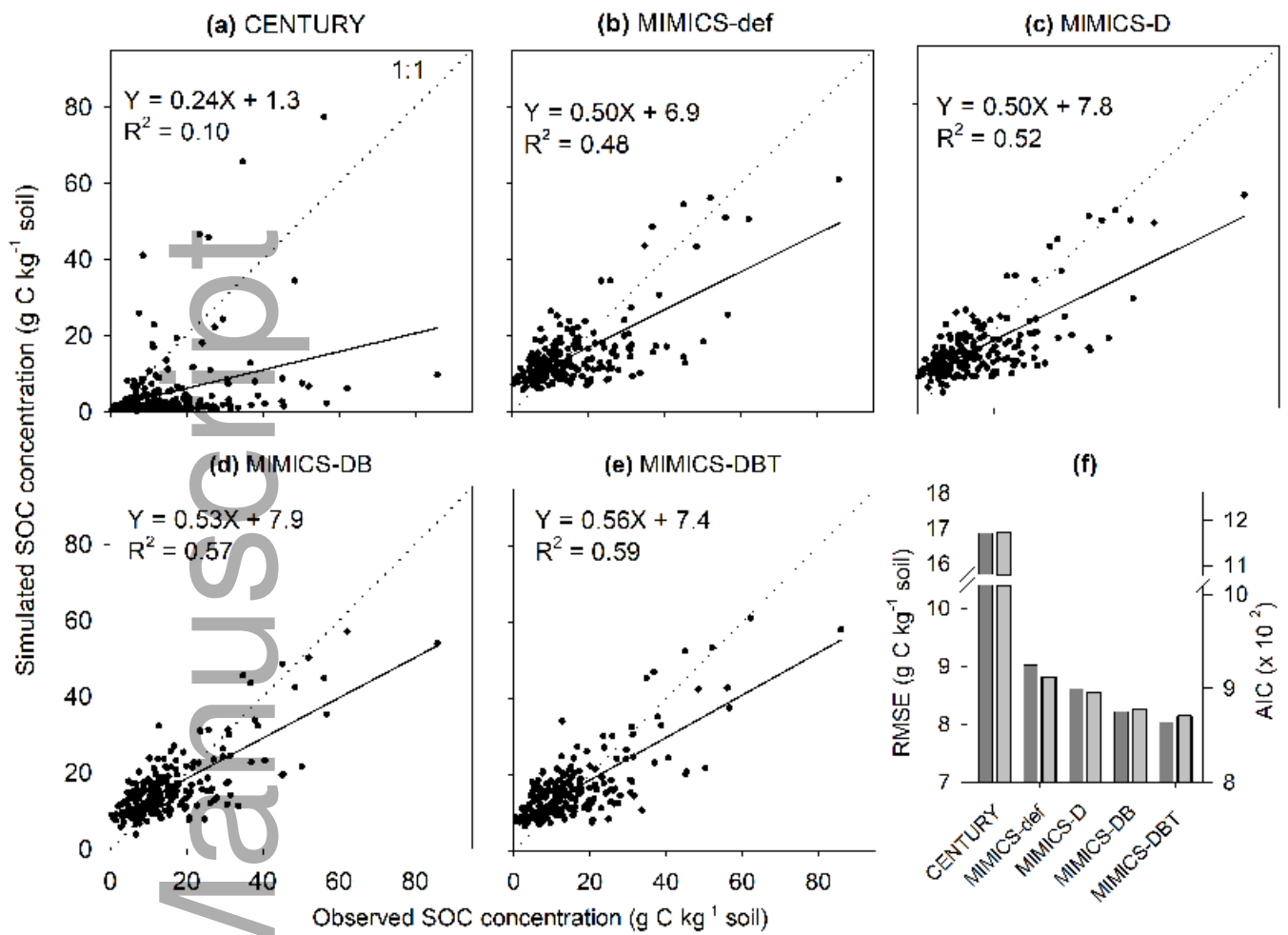
gcb_14994_f2.jpg
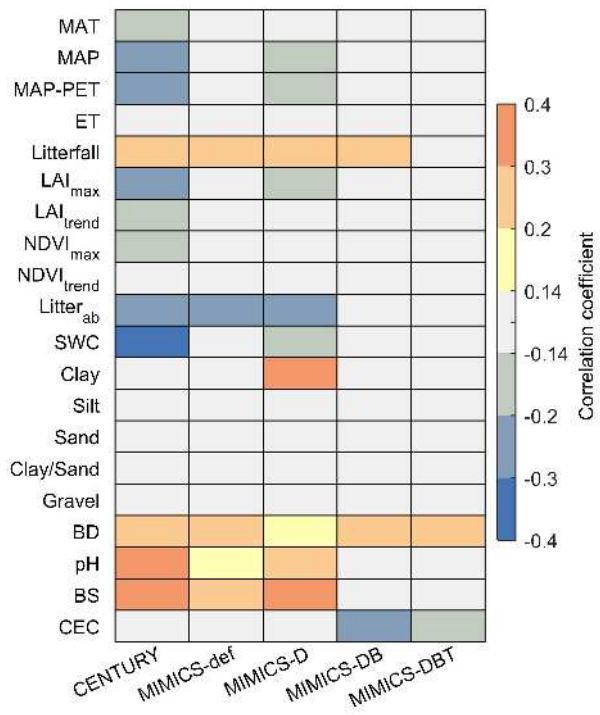
gcb_14994_f3.jpg
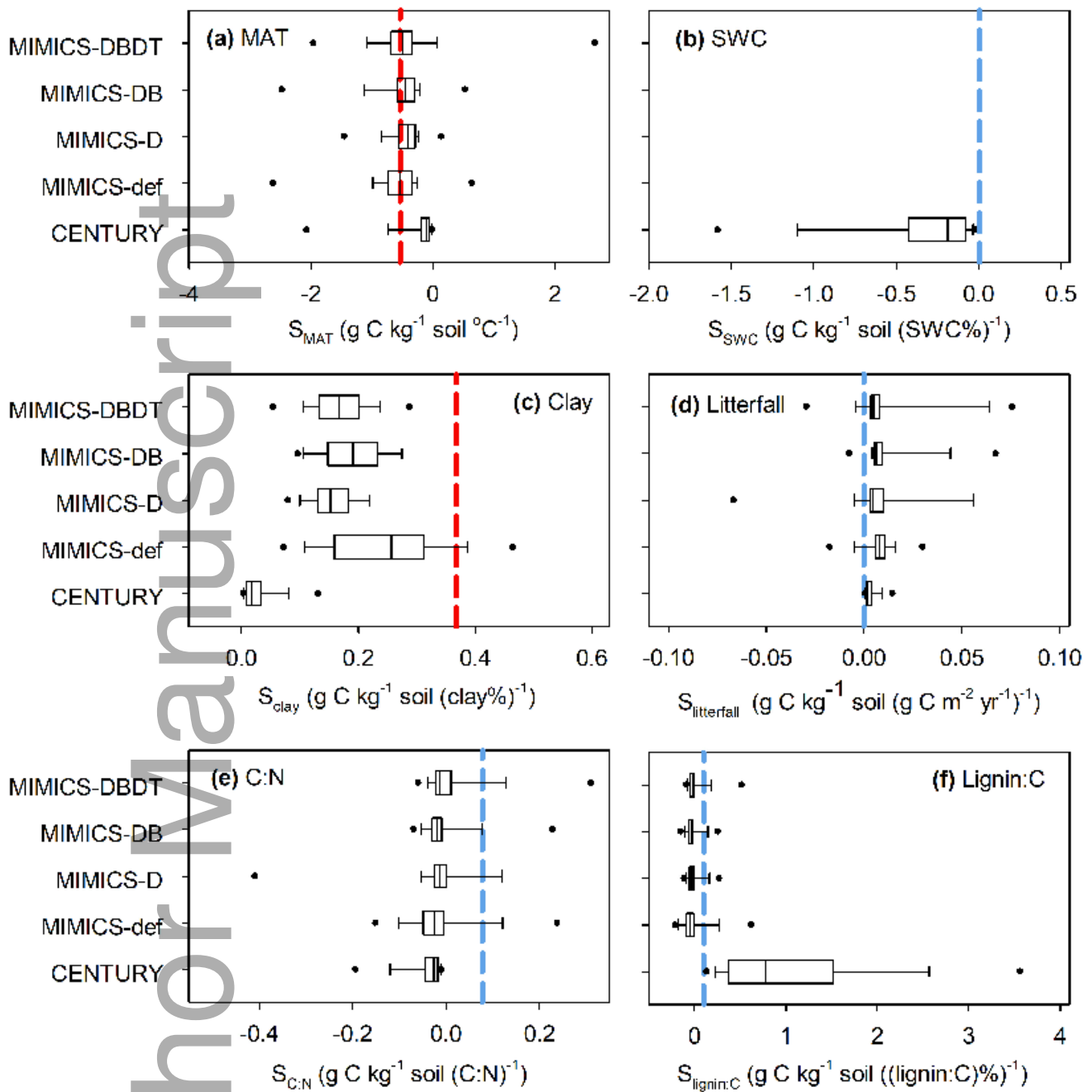
gcb_14994_f4.jpg

gcb_14994_f5.jpg

gcb_14994_f6.jpg

gcb_14994_f7.jpg